TURUN
YLIOPISTO
UNIVERSITY
OF TURKU

REVERSIBLE BASE-FILLING OF OLIGONUCLEOTIDES THROUGH FORMATION OF N-METHOXY-1,3-OXAZINANE AND -OXAZOLIDINE NUCLEOSIDES

Mark Nana Kwame Afari

TURUN YLIOPISTON JULKAISUJA – ANNALES UNIVERSITATIS TURKUENSIS
SARJA – SER. AI OSA – TOM. 741 | ASTRONOMICA – CHEMICA – PHYSICA – MATHEMATICA | TURKU 2025

TURUN
YLIOPISTO
UNIVERSITY
OF TURKU

REVERSIBLE BASE-FILLING OF OLIGONUCLEOTIDES THROUGH FORMATION OF N-METHOXY-1,3-OXAZINANE AND -OXAZOLIDINE NUCLEOSIDES

Mark Nana Kwame Afari

TURUN YLIOPISTON JULKAISUJA – ANNALES UNIVERSITATIS TURKUENSIS
SARJA – SER. AI OSA – TOM. 741 | ASTRONOMICA – CHEMICA – PHYSICA – MATHEMATICA | TURKU 2025

University of Turku

Faculty of Science
Department of Chemistry
Chemistry
Doctoral Programme in Exact Sciences (EXACTUS)

Supervised by

Professor Tuomas Lönnberg
Department of Chemistry
University of Turku
Turku, Finland

Professor Pasi Virta
Department of Chemistry
University of Turku
Turku, Finland

Reviewed by

Professor Kari Rissanen
Department of Chemistry
University of Jyväskylä
Jyväskylä, Finland

Associate Professor Hiromu Kashida
Department of Biomolecular Engineering
Nagoya University
Nagoya, Japan

Opponent

Professor Juan José Díaz Mochón
Department of Pharmaceutical and Organic Chemistry
University of Granada
Granada, Spain

ISBN 978-952-02-0258-3 (PRINT)
ISBN 978-952-02-0257-6 (PDF)
ISSN 0082-7002 (Print)
ISSN 2343-3175 (Online)
Painosalama, Turku, Finland 2025

Dedicated to my Lord and Saviour Jesus Christ,
my dear wife (Deborah Afari), family and friends

UNIVERSITY OF TURKU
Faculty of Science
Department of Chemistry
Chemistry
MARK NANA KWAME AFARI: Reversible Base-Filling of Oligonucleotides through formation of N-Methoxy-1,3-Oxazinane and -Oxazolidine Nucleosides
Doctoral Dissertation, 104 pp.
Doctoral Programme in Exact Sciences (EXACTUS)
August 2025

ABSTRACT

Dynamic combinatorial chemistry (DCC) has emerged as a powerful tool for screening and optimization of lead compounds for the discovery of new drugs. This thesis introduces a novel method for base filling through the reversible incorporation of nucleobase aldehydes into the backbone of modified oligonucleotides using the principle of DCC. The formation of N-methoxy-1,3-oxazinane (MOANA) and N-methoxy-1,3-oxazolidine (MOGNA) nucleoside analogues for the preparation of oligonucleotide conjugates has been systematically studied. The reaction involves the unprotected (2R,3S)-4-(methoxyamino)butane-1,2,3-triol (MABT) residue and nucleobase modified aldehydes. The reaction is reversible under slightly acidic conditions (pH 5.5) and affords highly stable products at pH 7.4, where the reaction effectively enters a "switched-off" state. The reaction rates and equilibrium constants were influenced by the structural variations of the aldehydes with observed half-lives ($t_{1/2}$) ranging from 9 to 32 hours. The reaction was predominantly driven by base stacking interactions and demonstrated significantly higher yield and base-pairing selectivity within the relatively rigid A-type double helices compared to the more flexible B-type double helices. In contrast, both single-stranded oligonucleotides and the Hoogsteen strand of triple helices exhibited significantly lower yield and selectivity for base-filling. The effects of the two isomers of the (2R,3S)-4-(methoxyamino)butane-1,2,3-triol scaffold on base-pairing selectivity were modest and varied depending on the sequence. This work is promising for the development of a modified oligonucleotides scaffold for reversible base filling which is important for the development of oligonucleotide therapeutics, diagnostics and DNA nanotechnology.

KEYWORDS: oligonucleotide, conjugation, base filling, base pairing, affinity, selectivity, oxazinane, oxazolidine

TURUN YLIOPISTO
Matemaattis-luonnontieteellinen tiedekunta
Kemian laitos
Kemia
MARK NANA KWAME AFARI: Oligonukleotidien reversiibeli täydentäminen emäksillä *N*-metoksi-1,3-oksatsinaani- ja -oksatsolidiininukleosidien muodostuksen kautta
Väitöskirja, 104 s.
Eksaktien tieteiden tohtoriohjelma (EXACTUS)
Elokuu 2025

TIIVISTELMÄ

Dynaamisesta kombinatorisesta kemiasta (DCC) on tullut tehokas työkalu johtoyhdisteiden seulontaan ja optimointiin uusien lääkkeiden löytämiseksi. Tämä väitöskirja esittelee uuden dynaamisen kombinatorisen kemian periaatteita hyödyntävän menetelmän, jossa muokattujen oligonukleotidien runko täydennetään reversiibelisti nukleoemästen aldehydijohdoksilla. *N*-Metoksi-1,3-oksatsinaani- ja -oksatsolidiininukleosidien muodostusta oligonukleotidikonjugaattien valmistamiseksi on tutkittu järjestelmällisesti. Reaktion lähtöaineina toimivat suojaamaton (2R,3S)-4-(meoksiamino)butaani-1,2,3-trioliyksikkö (MABT) ja nukleoemäs, johon on liitetty aldehydiryhmä. Reaktio on reversiibeli lievästi happamissa olosuhteissa (pH 5,5), mutta tuotteet ovat pysyviä pH:ssa 7,4, jolloin reaktio käytännössä pysähtyy. Reaktion nopeus ja tasapaino riippuivat käytettyjen aldehydien rakenteesta puoliintumisaikojen vaihdellessa 9:stä 32:een tuntiin. Pääasiallinen reaktiota ajava voima oli emäspinoutuminen ja reaktion saanto ja emäspariutumisselektiivisyys olivat huomattavasti korkeammat suhteellisen jäykillä A-tyypin kaksoiskierteillä kuin joustavammilla B-tyypin kaksoiskierteillä. Sitä vastoin yksinauhaisten oligonukleotidien ja kolmoiskierteiden Hoogsteen-nauhan emäksillä täydentämisen saanto ja selektiivisyys olivat selvästi heikommat. (2R,3S)-4-(meoksiamino)butaani-1,2,3-triolirungon paikkaisomerian vaikutus emäspariutumisselektiivisyyteen oli vähäinen ja oligonukleotidin sekvenssistä riippuva. Väitöskirjatyö on lupaava sellaisten muokattujen oligonukleotidien kehittämiseksi, joiden runkoa voidaan reversiibelisti täydentää emäksillä. Nämä puolestaan olisivat hyödyllisiä kehitettäessä oligonukleotidilääkkeitä, diagnostiikkaa ja DNA-nanoteknologiaa.

ASIASANAT: oligonukleotidi, konjugaatio, emäksillä täydentäminen, emäspariutuminen, affiniteetti, selektiivisyys, oksatsinaani, oksatsolidiini.

Table of Contents

Abbreviations

ASOs	Antisense Oligonucleotides
CD	Circular Dichroism
CDS	Coding Sequence
circRNA	Circular RNA
CRISPR-Cas9	Clustered Regularly Interspaced Short Palindromic Repeats-associated protein 9
CPG	Controlled Pore Glass
DCC	Dynamic Combinatorial Chemistry
DCL	Dynamic Combinatorial Library
DMF	N,N-dimethylformamide
DMSO	Dimethylsulfoxide
DMTrCl	4,4'-Dimethoxytrityl Chloride
DNAzymes	Deoxyribozymes or DNA Enzymes
dNTPs	Deoxynucleotidyl triphosphates
DyNAs	Side-chain Dynamic Nucleic Acids
ESI-MS-TOF	Electrospray Ionization Mass Spectrometry coupled with Time-of-Flight
Fmoc	Fluorenylmethoxycarbonyl
GC	Gas Chromatography
HRMS	High Resolution Mass Spectrometry
HG bps	Hoogsteen base pairs
lncRNA	Long Non-Coding RNA
LCMS	Liquid Chromatography Mass Spectrometry
MABT	(2R,3S)-4-(methoxyamino)butane-1,2,3-triol
MOANA	N-methoxy-1,3-Oxazinane Nucleic Acid
MOGNA	N-Methoxy-1,3-Oxazolidine Glycol Nucleic Acid
miRNA	MicroRNA
NMR	Nuclear Magnetic Resonance
2'-OMe RNA	2'-O-methyl Ribonucleic Acid
PCR	Polymerase Chain Reaction
PNA	Peptide nucleic acids

piRNA	Piwi-Interacting RNA
RCA	Rolling circle amplification
RP-HPLC	Reverse-Phase High-Performance Liquid Chromatography
saRNA	Small Activating RNA
SEC	Size Exclusion Chromatography
shRNA	Short Hairpin RNA
siRNAs	small interfering RNAs
TBDMSCl	tert-Butyldimethylsilyl Chloride,
TFOs	Triplex-Forming Oligonucleotides
TEAA	Triethylammonium acetate
tmRNA	Transfer Messenger RNA
Tm	melting temperature
UPLC-TOF-MS	Ultra-Performance Liquid Chromatography coupled with Time-of-Flight Mass Spectrometry

List of Original Publications

This dissertation is based on the following original publications, which are referred to in the text by their Roman numerals:

I Mark N. K. Afari, Pasi Virta, and Tuomas Lönnberg; N-Methoxy-1,3-Oxazinane Nucleic Acids (MOANAs) – a Configurationally Flexible Backbone Modification Allows Post-Synthetic Incorporation of Base Moieties, *Org. Biomol. Chem.* **2022**, *20*, 3480-3485.

II Mark N. K. Afari, K. Nurmi, P. Virta, and T. Lönnberg; Watson-Crick Base Pairing of N-Methoxy-1,3-Oxazinane (MOANA) Nucleoside Analogues within Double-Helical DNA, *ChemistryOpen,* **2023**, *12*, e202300085.

III Mark N. K. Afari, Ninna Heikinmäki, Pasi Virta, and Tuomas Lönnberg; The Impact of Secondary Structure on the Base-Filling of N-Methoxy-1,3-Oxazinane (MOANA) and N-Methoxy-1,3-Oxazolidine Glycol Nucleic Acid (MOGNA) Oligonucleotides, *ChemBioChem*, **2024**, *26*, e202400666.

List of other related publications

I Mark N. K. Afari, Tuomas Lönnberg, Base-Filling in Double-Helical Nucleic Acids, *ChemistryOpen,* **2024**, *13*, e202400088.

1 Introduction

1.1 Nucleic acids

Nucleic acids are natural biopolymers found universally in the cells of living organisms. They are not only responsible for transmitting genetic information but also play additional functional roles[1,2] within biological systems such as regulate transcription and translation, modulate chromosomal structure, catalyze protein synthesis and control protein function.[3–7] There are two primary types of nucleic acids: deoxyribonucleic acid (DNA) and ribonucleic acid (RNA). These two types differ in both structure and function. DNA is typically found in a double helical structure, where two complementary strands are joined together by hydrogen-bonded base pairs (Figure 1A). In contrast, RNA (Figure 1C) is usually a single-stranded polyribonucleotide chain, but it can also form a double helix with a complementary sequence.

For nucleic acids to perform various biological activities they need to adopt several alternative conformations beyond their classical forms.[8] For instance, under specific conditions, DNA sequences can fold into non-B-form secondary structures such as triplexes,[9,10] cruciforms[11–13] tetraplexes (eg. G-quadruplex)[14–16] and left-handed double helices.[17–19] Similarly, non-canonical RNA structures, including hairpins, bulged duplexes and RNA quadruplexes are known to serve as additional endogenous regulators of cellular functions.[20–24] The non-canonical forms of nucleic acids are responsible for genetic alterations that lead to various infectious diseases, genetic disorders, neurological conditions, and cancers.[25–28]

Naturally occurring nucleic acids are made up of monomeric building blocks called nucleotides. Each nucleotide consists of a sugar moiety, a phosphate group and one of five nitrogenous bases (Figure 1B). The nitrogenous bases are classified into two main groups: **pyrimidines** and **purines**. Pyrimidine bases include cytosine (C), thymine (T) found only in DNA, and uracil (U) found only in RNA. Purines consist of adenine (A) and guanine (G). These bases form N-glycosidic bonds between the N1 atom of pyrimidines or the N9 atom of purines and the C1' carbon of the pentose sugar.

A key distinction between DNA and RNA lies in their sugar units: DNA contains a 2-deoxyribose sugar moiety, whereas RNA has a ribose moiety. Nucleotides are

connected together in an array by 5',3'-phosphodiester bonds between two sugar moieties, creating an alternating sugar-phosphate backbone. When the phosphate group of a monomer is absent, the molecule is referred to as a nucleoside. The phosphodiester groups in nucleic acids are anionic and stable under physiological conditions. A short sequence of nucleotides, typically consisting of 8 to 50 units, is called an oligonucleotide.

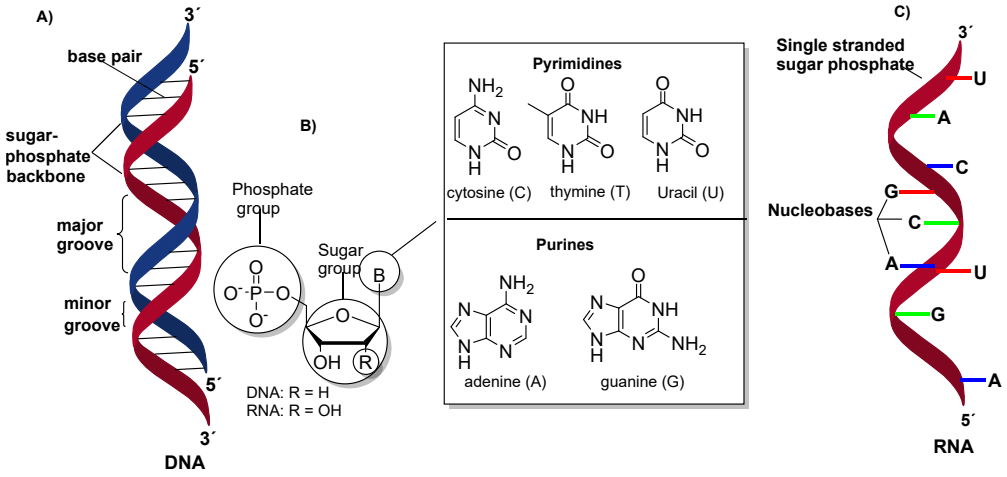

Figure 1. **A**) Structure of DNA double helix, **B**) nucleotides (DNA when R = H, RNA when R = OH), and **C**) Structure of single stranded RNA

1.2 Biological relevance of DNA and RNA

DNA is often referred to as the blueprint for life. According to the central dogma of molecular biology, DNA contains the genetic information that is transcribed into RNA and RNA is responsible for the conversion (translation) of this information into the assembly of a protein. RNA is a versatile molecule playing a crucial role in various biological pathways. The functions of RNA can be broadly classified as either translated (protein-coding) or untranslated (non-coding). Messenger RNA (mRNA), a protein-coding RNA, plays a key role in the flow of genetic information within the central dogma. It conveys the genetic information from the DNA in the nucleus of the cell to the ribosomes in the cytoplasm where it serves as a template for protein synthesis. A matured translatable mRNA sequence consists of the coding sequence (CDS), surrounded by untranslated regions (UTRs).

The other RNA molecules, called noncoding RNAs (ncRNAs), do not encode proteins, however, they play a multitude of important roles in every cell. NcRNAs are the final functional transcripts of DNA. There are several different types of ncRNA. Ribosomal RNA (rRNA) catalyzes peptide bond formation between two

amino acid residues. Transfer RNA (tRNA) helps to facilitates the accurate arrangement of amino acids into a polypeptide chain according to the sequence specified by mRNA. Small nuclear RNAs (snRNAs)[29,30] act as catalysts that splice mRNA into its mature form and are important in the selection of alternative splicing sequences. Small nucleolar RNAs (snoRNAs)[31–34] are bound to four core proteins and act as guides to correctly target modifications for the maturation of rRNA. Other ncRNAs include long non-coding RNA (lncRNA),[35,36] short hairpin RNA (shRNA), micro-RNA (miRNA),[37–39] transfer messenger RNA (tmRNA), small interfering RNA (siRNA),[40–42] small activating RNA (saRNA), piwi-interacting RNA (piRNA),[43–45] circular RNA (circRNA), ribozymes, and exosomal RNA.[46–48]

1.3 Watson-Crick base pairing

Classical Watson-Crick base pairs (WC bps) are formed by specific hydrogen bonding interactions between two of the four nitrogenous bases (A, C, G, T/U) of DNA and RNA. Adenine interacts with thymine in DNA or uracil in RNA while guanine associates with cytosine. The A-T/U pairs form through two hydrogen bonds that involve N1(A)…H-N3(T/U) and N6(A)-H…O4(T/U) and the G-C base pairs by three such interactions (N1(G)-H…N3(C), N2(G)-H…O2(C) and O6(G)…H-N4(C). The additional hydrogen bond of the G-C base pair results in higher melting temperature of G-C over A-T rich sequences. The estimated free energy for isolated A-T and G-C base pairs is approximately -13 kcal/mol and -21 kcal/mol, respectively. [49–51] Furthermore, G-C base pairs are usually closer to the ideal planar geometry than A-T base pairs.

The electrostatic nature of hydrogen bonding brings the protons of one base in close proximity to the nitrogen and oxygen acceptors of the complementary base, with distances between 1.9-2.0 Å, which is much closer than the typical van der Waals separation of 2.7-2.8 Å. In each purine-pyrimidine pair, the bases lie in a common plane, maintaining a constant distance of approximately 10.5 Å between the C1' sugar atoms. The C1'-C1' vector forms equivalent angles (around 55°) with the glycosidic bonds (C1'-N9 in purines and C1'-N1 in pyrimidines). The complementary base pairing rules of A-T (or A-U in RNA) and G-C (Figure 2) enable the formation of a stable double-stranded structure of an arbitrary base sequence, thus facilitating accurate copying of the genetic information from DNA to RNA.

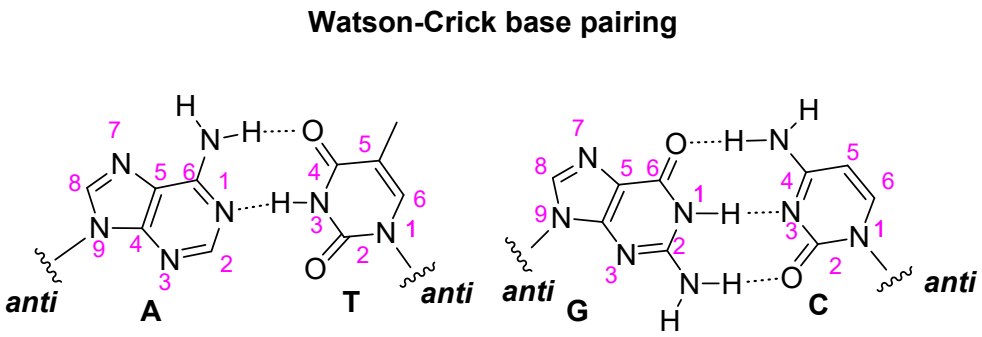

Figure 2. Base pairing modes: Watson-Crick base pairing.

1.4 Hoogsteen base pairing

Bases do not always pair according to the Watson–Crick base pairing rule. Hoogsteen base pairs (HG bps) provide an alternative pairing geometry (Figure 3). It was discovered by Karst Hoogsteen in 1959, when he was investigating the pairing of 1-methylthymine and 1-methyladenine by single crystal X-ray crystallography.[52] Although Watson-crick base pairing has become the dominant model for A-T and G-C bps in DNA, HG bps continue to surface in high-resolution structures of antiparallel DNA duplexes[53] and DNA in complex with quinoxaline and proteins[54,55]. Differentiating between Hoogsteen and Watson-Crick base pairs in large DNA assemblies and complexes using traditional biological techniques is often challenging.

Computational studies have proven that the stability of antiparallel HG duplex is comparable to the B-form WC helix and that the chimeric WC-HG helix is an energetically accessible conformation.[56,57] Parallel studies using NMR and circular dichroism (CD) [58–60] have indicated that A-T and G-C+ HG bps can be found in parallel double stranded DNA, dumbbell-like DNA structures and DNA triplexes[61,62]. In duplex DNA, HG bps can be formed by rotating the purine base 180° around the glycosidic bond to adopt a *syn* conformation instead of *anti*-conformation. While the A-T HG bps retain the A-N6-H-O4-T H-bond, they substitute the N1-H-N3 H-bond with an N7-H-N3 H-bond. G-C HG bps, in turn, retain the O6-H-N4 H-bond and substitute the other two WC H-bonds (N1-H-N3 and N2-H-O2) with a single N7-H-N3+ H-bond which needs the protonation of cytosine N3. Additionally, formation of HG-type H-bonds requires that the two bases come into closer proximity which constricts the C1′-C1′distance by approximately 2 Å relative to WC bps.[63] Hoogsteen base pairs are less stable than Watson–Crick base pairs by 0.22 to 0.64 kcal/mol depending on the ionic conditions and the specific base composition. The HG bp A-T is as stable as the G-C^+ base pair at low pH in the presence of Mg^{2+} ions.

The structural modification of sequence information in duplex DNA, particularly through Hoogsteen base pairs (HG bps), allows for the execution of unique and specialized functions. [64–66] Hoogsteen base pairing allows the formation of triple-helix DNA (triplex or *H-DNA)*. Although HG bps are rare compared to WC, they play a crucial role in replication by DNA polymerase,[67,68] DNA repair enzymes[69–71], recognition by transcription factors[72–74] and binding to small molecules.[75] Hoogsteen base pairs are primarily found in higher-order nucleic acid secondary structures, such as triplexes and quadruplexes, and are only rarely observed in the context of double helices.[76,77]

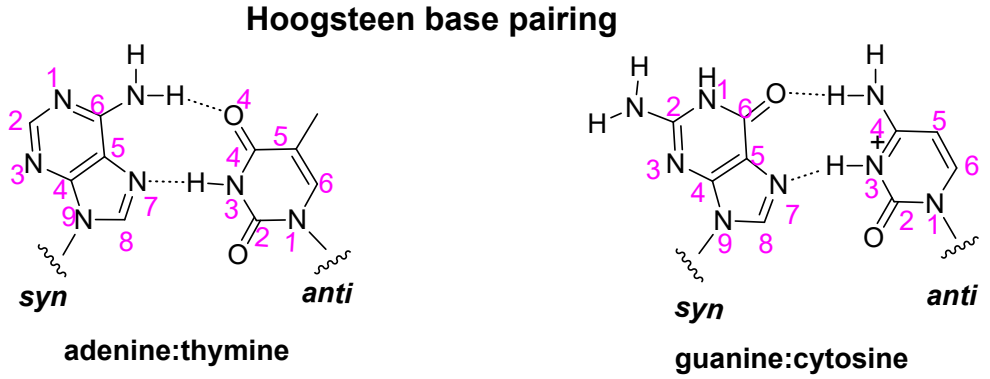

Figure 3. Base pairing modes: Hoogsteen base pairing.

1.5 Base stacking interactions

Base stacking interactions, also known as π–π stacking interactions, are non-covalent interactions between aromatic moieties. Base stacking is a key force that contributes to the stability of the three-dimensional structure of RNA and DNA,[78] often more so than base pairing. Base stacking relies on several non-covalent interactions, including electrostatic attraction between dipoles, van der Waals forces and solvation effects.[79,80] The strength of stacking interactions increases in the order of pyrimidine-pyrimidine, purine-pyrimidine, and purine-purine. This is due to the larger surface area and higher polarizability of purines.[81–84]

Measuring the stabilizing effect of unpaired bases enables direct quantification of stacking interactions without interference from base pairing. In RNA, base stacking at the 3′-terminus is more energetically favorable than at the 5′-terminus, whereas in DNA the opposite is true. Base stacking in the middle of either the DNA or RNA double helix exerts a greater influence on stability compared to stacking at the termini. However, the overall effect is complex due to factors such as the rigidity of the helix and the cooperative nature of base stacking interactions. Stacking

interactions play a crucial role in metabolic processes, the design of aptamers, and the construction of hierarchical DNA nanostructures.

1.6 Oligonucleotide modifications

Recently, there has been growing interest in the use of modified oligonucleotides.[85–87] DNA and RNA oligonucleotides have been widely used as tools in antisense, aptamer and antigene therapy etc. Chemical modifications to the backbone, sugar, and nucleobase of oligonucleotides, as well as conjugation or derivatization of modified oligonucleotides (Figure 4), have significantly addressed longstanding challenges associated with native nucleic acids. These advancements have enhanced nuclease resistance, bioavailability, specificity, binding affinity, biodistribution, cell targeting, and immune response.[88–90] For instance, modifying the sugar unit can enhance binding affinity and improve nuclease stability and/or interactions with cellular proteins.[91] Modifications to nucleobases can improve base-pairing specificity, and adjustments to the phosphodiester backbone can boost nuclease resistance and optimize pharmacokinetic properties.[92,93] Additionally, conjugation with lipophilic or cell-targeting moieties can improve tissue targeting and protein-binding properties.[94]

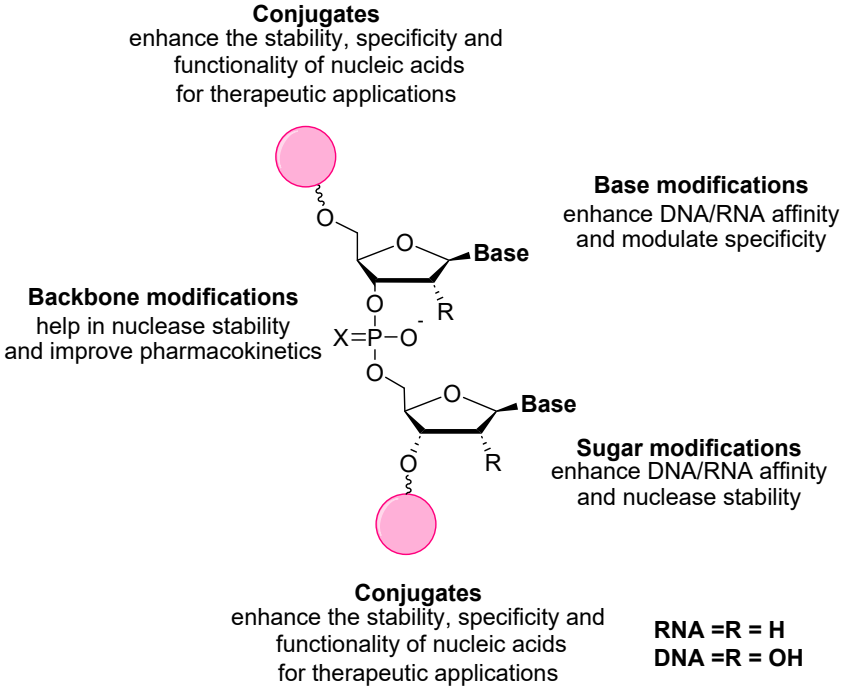

Figure 4. Chemical modifications of therapeutic oligonucleotides.

1.6.1 Sugar modification

The (deoxy)ribofuranose sugar (Figure 5) conformation plays a crucial role in the structure and function of nucleic acids. Over the years, several modifications have been incorporated into the sugar moieties to improve their therapeutic potential. The stability of oligonucleotide duplexes and the formation of stable functional protein-oligonucleotide complexes is largely influenced by the conformation and dynamics of the sugar moiety. For instance, replacing the 2'-hydroxy group with methoxy or fluoro groups has proven advantageous for the development of antisense oligonucleotides (AONs), small interfering RNAs (siRNAs), aptamers, microRNAs, and CRISPR-Cas9 systems.[95,96] Incorporating a 2'-SCF_3[97] group into the sugar moiety enables the monitoring of nucleotides by ^{19}F NMR at micromolar concentrations, although this modification significantly destabilizes the double helix. Furthermore, 2'-$SeCH_3$[98] and 2'-N_3[99] nucleotides have also been developed, expanding the toolkit for functional nucleotide modification. Beyond 2' modifications, 4' modifications such as substituting the endocyclic oxygen with NAc[100], CH_2,[101] S,[102] or Se[98]have shown significant utility in gene-based therapies and crystallographic studies.

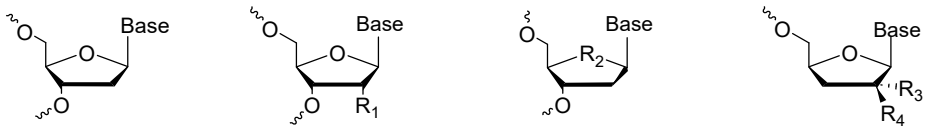

Figure 5. Examples of pentose sugar mimic: modification at 2', 4' and a sugar with an expanded ring. The structure on the left shows the canonical deoxyribose. R_1 = F, OMe, SCF_3, SeMe, N3. R_2 = CH_2, NAc, S, Se. R_3 = OH, F, R_4 = F.

1.6.2 Base modification

Natural nucleobases, whether purines or pyrimidines, can be modified to enhance stability through various mechanisms. These include hydrogen-bonding interactions, hydrophobic forces, stacking effects and metal-mediated bonding. Such modifications are achieved by incorporating additional functional groups[103–108], inserting extra rings[109–111], or attaching a linker[107,108] between the sugar and the base. Various analogues have been developed to enhance the functionality of nucleobases.[112] These modifications generally cause minimal disruption to Watson-Crick base pairing, allowing the flow of genetic information to remain unaffected. Additionally, nucleobase analogues can introduce properties such as redox activity[113], fluorescence,[114] and even anti-cancer or antiviral activity.[115,116]

The genetic alphabet has been expanded through the development of unnatural base pairs (UBPs). These synthetic base pairs are designed for use in both *in vitro* and *in vivo* systems, paving the way for innovative next-generation biotechnologies. For instance, the hydrogen-bond-mediated isoG-isoC pair (Figure 6A) serves as a constitutional isomer of the G-C pair, conforming to a different hydrogen-bond geometry than natural base pairs.[117,118] In addition to hydrogen-bond-mediated unnatural base pairs (UBPs), non-hydrogen-bonded hydrophobic bases (Figure 6B) have emerged as promising candidates. Base pairing can also be facilitated by metal ions. Metal-mediated base pairs (Figure 6C) can compensate for the absence of hydrogen bonds, imparting new properties to the DNA double helix and expanding its potential applications. In early 1963, mercury(II) was incorporated between thymine (T) bases.[119] Recently, metal-mediated base pairs have gained significant attention, leading to the development of various novel systems.[120] For instance, copper(II) has been used to connect hydroxypyridone bases[121] and silver (I) to connect pyridine bases within the DNA double helix.

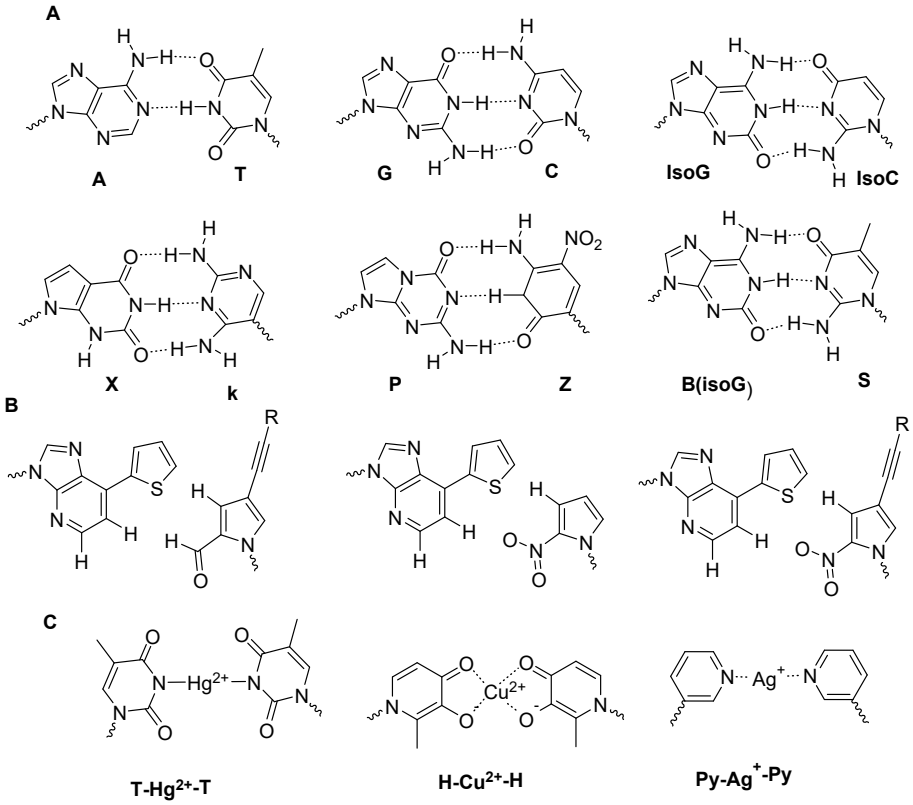

Figure 6. Structures of A) H-bond mediated natural and unnatural base pairs, B) hydrophobic unnatural base pairs, C) metal-mediated unnatural base pairs.

1.6.3 Phosphate modification

The phosphodiester backbone of nucleic acids is highly susceptible to hydrolysis by nucleases under biological conditions, limiting its effectiveness for therapeutic applications. Significant efforts have been made to explore alternative backbones that enhance stability against nucleases and improve affinity for RNA/DNA.[122] Common backbone modifications involve substituting one of the non-bridging oxygen atoms in the phosphate linkage with boron, nitrogen, carbon, or sulfur, as illustrated in Figure 7. These alterations significantly impact the physicochemical and biological properties of oligonucleotides. For example, replacing a non-bridging oxygen with sulfur creates a phosphorothioate linkage, which carries a negative charge and enhances nuclease stability while retaining chemical stability similar to the conventional PO linkage.[123] Conversely, substituting oxygen with carbon leads to the formation of an alkyl phosphonate linkage, which is neutral in charge, reduces affinity for RNA and is unstable under basic conditions, particularly during the deprotection steps following oligonucleotide synthesis.[124] Replacing oxygen with nitrogen neutralizes the charge and reduces the affinity for RNA and the resulting phosphoramidate linkage is highly unstable in the acidic environment required to remove the dimethoxytrityl protecting group during synthesis.[125] Substituting the anionic oxygen with an alkoxy group results in a phosphotriester linkage, which is also neutral and labile under basic conditions necessary for the deprotection of oligonucleotides post-synthesis. Boranophosphate is another interesting modified backbone structure in which one of the non-bridging oxygen atoms in the phosphate group is replaced with a borane group (-BH_3). Finally, several backbone modifications have been reported that replace one of the bridging oxygen atoms in the phosphate (PO) linkage with either nitrogen (N in 3′-phosphoramidates) or carbon (C in 3′-methylene phosphonates).[126]

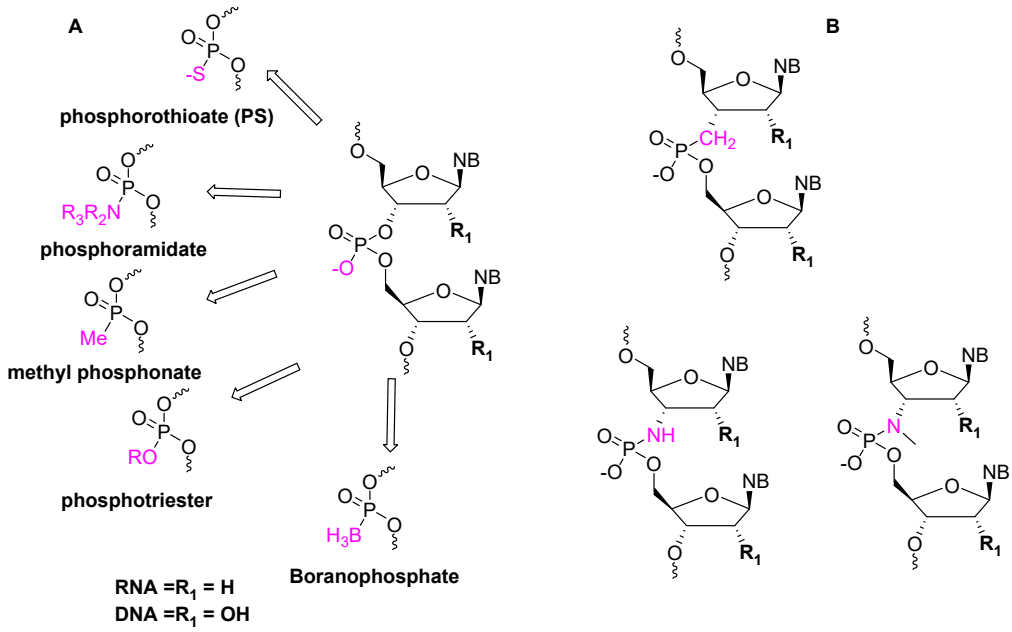

Figure 7. Examples of backbone modifications of nucleic acids analogues.

1.7 Chemical and enzymatic synthesis of modified DNA

DNA can be chemically modified through solid-phase synthesis or enzymatically using DNA polymerases in combination with unnatural deoxynucleotidyl triphosphates (dNTPs). Solid-phase synthesis is widely employed for producing large quantities of oligonucleotides. However, it has limitations, including a maximum synthesis length of approximately 200 nucleotides and constraints related to the compatibility of functional groups with the chemical reactions used in oligonucleotide assembly.[127] Enzymatic DNA modification methods include PCR, primer extension, and rolling circle amplification (RCA). These techniques rely on polymerases with limited tolerance for chemically modified dNTPs and require a template strand to guide primer extension.

1.7.1 Direct incorporation of modifications by solid phase oligonucleotide synthesis

For the direct incorporation, the functional group is first introduced into a predetermined position of the nucleotide scaffold, which is then attached to DNA directly through a synthetic cycle. The most commonly used technique for robust and efficient chemical synthesis of oligonucleotides is automated solid-phase

synthesis, which involves a four-cycle process on solid support (Scheme 1).[128] In this approach, large excesses of reagents are employed to rapidly drive reactions to completion, with unreacted reagents easily washed away. The initial building block is attached to solid support via a long-chain alkylamine (LCAA) linker, connected through a succinyl spacer. This attachment provides a stable foundation for the subsequent stepwise addition of nucleotides. The synthesis proceeds in the 3′ to 5′ direction. Initially, the 5′-O-DMTr protecting group of the support-bound nucleoside is removed using an acid. The resulting 5′-hydroxy group is then allowed to react with a nucleoside phosphoramidite monomer in the presence of an activator, typically tetrazole or one of its derivatives. The unreacted 5′-hydroxy groups are blocked in a capping step, where acetylation is achieved using acetic anhydride, *N*-methylimidazole, and pyridine. The subsequent oxidation step converts the reactive P(III) phosphorus atom of the phosphite triester, formed during coupling, into a stable P(V) form. This step is accomplished using iodine in the presence of water and pyridine. This entire cycle is repeated, adding a nucleotide at each step until the desired oligonucleotide is synthesized. The phosphoramidite coupling step is highly sensitive to moisture so the reaction must be conducted under a nitrogen or argon atmosphere and with anhydrous solvents. The efficiency of each cycle can be monitored during the detritylation step when the 4,4′-DMTr cation is removed. After the final cycle and detritylation, treatment with concentrated aqueous ammonia is performed to cleave the oligonucleotide from the solid support and remove the base protecting groups and the cyanoethyl groups on the phosphates. The direct incorporation of functional molecules into a desired position within a DNA sequence presents significant challenges. One major difficulty is the synthesis of a corresponding phosphoramidite monomer for unnatural molecules, which is often complex and challenging. Additionally, certain functional groups in phosphoramidite building blocks may be incompatible with the oxidation step in the DNA synthesis cycle. Given these limitations, a post-synthetic approach emerges as an attractive alternative.

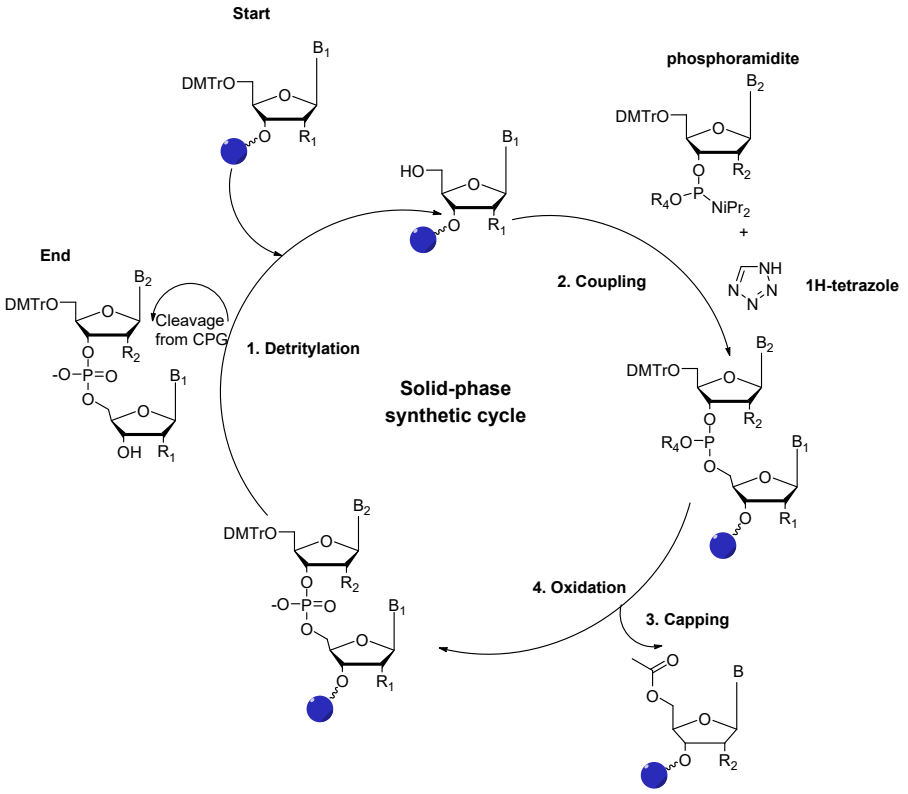

Scheme 1. General scheme of DNA/RNA solid-phase synthetic cycle using the phosphoramidite approach. R_1, and R_4: protecting groups for 5′-OH, 2′-OH, phosphate residue, respectively; R_2 (H or OH). Conditions: 1) Detritylation, 3% TCA, dichloromethane (DCM) 2) Coupling, 0.25 M tetrazole (or DCI), phosphoramidite, acetonitrile (ACN) 3) Capping, Ac_2O, N-methylimidazole, pyridine, ACN 4) Oxidation, 0.02 M I_2, pyridine, H_2O, tetrahydrofuran (THF).

1.7.2 Enzymatic synthesis via DNA polymerases

DNA polymerases[129] are a class of enzymes that catalyze the synthesis of polydeoxyribonucleotides from deoxyribonucleoside triphosphates (dNTPs). They play a fundamental role in DNA replication, repair, and, in some cases, cell differentiation. Under appropriate conditions, DNA polymerases can also be used for *in vitro* DNA synthesis. A primer is an initiating oligonucleotide (or polynucleotide) with a free 3′ hydroxy group, which serves as the starting point for DNA strand elongation. Primers provide a double-stranded structure by annealing to a complementary region of an RNA or DNA template. The enzyme then extends the primer in the 5′ → 3′ direction, following the Watson–Crick base-pairing rule, where A pairs with T (or U in RNA), and C pairs with G. This process occurs in a repetitive

cycle which involves nucleotide binding, base pairing, phosphodiester bond formation and template strand progression.

DNA polymerases exhibit remarkable speed and accuracy, synthesizing DNA at a rate of nearly 1,000 base pairs per second,[130] with an error frequency of only one mistake per million base pairs.[131,132] A key limitation of enzymatic DNA synthesis is the strict substrate specificity of DNA polymerases, which limits the incorporation of chemical modifications into oligonucleotides. As a result, post-synthetic functionalization is often required for many applications. Additionally, enzymatic synthesis becomes less efficient for generating long or highly modified DNA sequences due to polymerase errors and premature termination.

1.7.3 Post-Synthetic Functionalization of Nucleic Acids

Post-synthetic functionalization[133] of DNA (Scheme 2) is the technique of modifying nucleic acids after they have been synthesized, either chemically or enzymatically as described above. This technique allows the introduction of functional groups, probes, or modifications that are difficult or impossible to incorporate during direct synthesis and reduces the synthetic challenges by reducing monomer complexity. There are some simple small functional handles, such as linear alkynes, cycloalkynes, aldehydes, carboxylic acids, primary amines[134] or thiols[135] which can be introduced as nucleobase modifications during enzymatic or chemical synthesis, and subsequently reacted to generate the final desired modification. For others, such as azides, a second pre-labelling step is sometimes necessary because of the chemical instability during solid-phase oligonucleotide synthesis. Reactions widely employed for post-synthetic functionalization include oxime and hydrazone,[136–141] ester modification,[142], peptide coupling conjugation,[143,144] click chemistry[145], Diels—Alder reaction[146] and Staudinger ligation.[147]

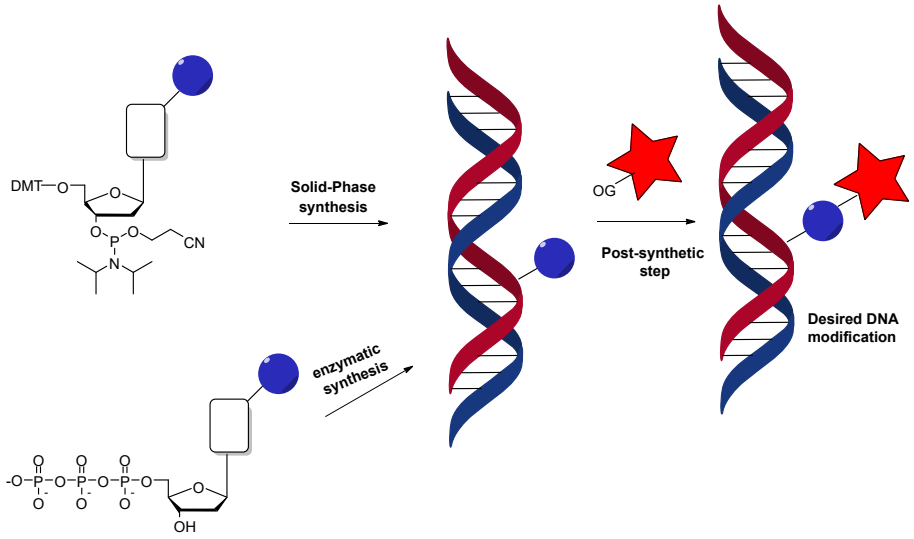

Scheme 2. Post-synthetic functionalization of DNA.

1.8 Dynamic combinatorial chemistry

Combinatorial chemistry has evolved into a powerful technology for generating vast numbers of structurally related compounds. Unlike classical organic synthesis, which follows a sequential approach where a target molecule is synthesized step by step to yield a single product, combinatorial chemistry employs a parallel strategy, enabling the simultaneous synthesis of multiple compounds using different reactants (Scheme 3). Moreover, combinatorial steps can also be performed sequentially, further expanding the diversity of potential products. Combinatorial chemistry was initially developed for creating peptide libraries to screen against antibodies and identify receptors with optimal binding characteristics and has since expanded significantly and is now a cornerstone technique in drug discovery. Various methodologies have been devised for chemical library generation.

Dynamic combinatorial chemistry (DCC) is a powerful screening tool that harnesses the reversible assembly of molecular building blocks through covalent and non-covalent bonds,[148–151] creating dynamic combinatorial libraries (DCLs) of potentially complex, interchanging products with high efficiency. As the reactions between the monomeric building blocks are reversible, the distribution of products is governed by their thermodynamic stability. DCLs have an advantage over traditional combinatorial libraries, as the addition of a target molecule can drive the library's composition to re-equilibrate, selectively amplifying members with the strongest affinity for the target. This process allows for the identification of the best binders without the need for conventional synthesis, purification, and characterization of each individual library member. DCLs have a wide range of

applications, including receptor design[152–155], catalysis[156,157], drug discovery[158,159], dynamic resolution[160], self-sorting[161], self-replication[162,163], DNA-templated synthesis[164,165], sensing[166,167], and the controlled release of bioactive compounds.[168,169]

The distribution of dynamic combinatorial libraries (DCLs) depends on the composition and intrinsic reactivity of the building blocks [170,171], as well as the thermodynamic stability of each member of the library under the given experimental conditions. The DCL is responsive to external stimuli. In the absence of external stimuli, the building blocks engage in reactions that generate all possible combinatorial products once equilibrium is achieved. However, when external stimuli are introduced, the equilibrium becomes biased and shifts, altering the product distribution within the library. The stimuli can be changes in pH[172,173] or temperature[174,175], exposure to light[176,177], the addition of metal ions[178,179], reversible phase separation[180], mechanical forces[181], gelation[182] or an electric field.[183,184] Also, a biological template such as a peptide[158] or a protein[185] can influence the composition of the library. Additionally, solid-state DCC often produces libraries with compositions different from those achieved through equilibration in solution.[186]

The composition of a DCL can be analyzed using high performance liquid chromatography (HPLC)[187–189], size-exclusion chromatography (SEC)[190], gas chromatography (GC)[191] and mass spectrometry (MS)[192–194]. When the target (e.g. a protein) can be subjected to non-denaturing electrospray ionization mass spectrometry (ESI-MS)[195,196], both the stoichiometry and binding strength to the target can be measured. In cases where the DCL contains a limited number of components, techniques such as X-ray crystallography[197,198], nuclear magnetic resonance (NMR) spectroscopy[199,200], and circular dichroism (CD) spectroscopy [201] have been utilized for analysis.

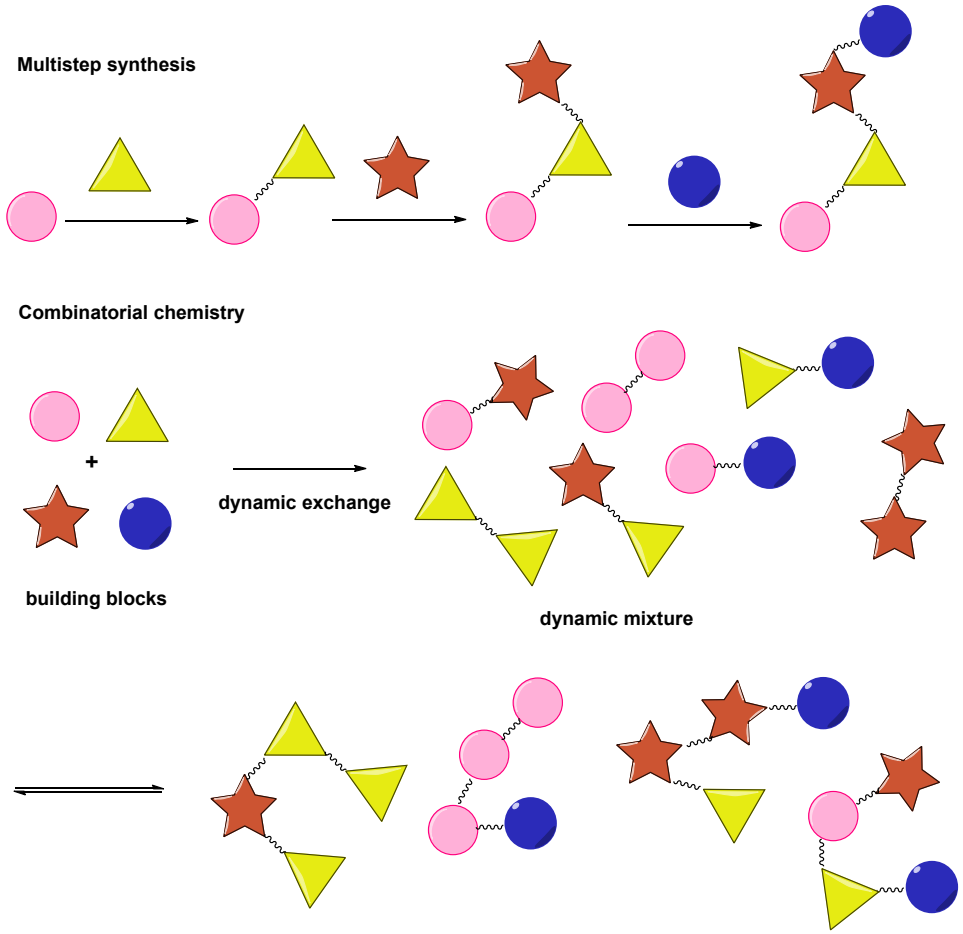

Scheme 3. Comparison of classic organic synthesis and dynamic combinatorial chemistry.

1.8.1 Conditions for formation of dynamic combinatorial libraries

The main feature of DCC is the reversible reaction that allows exchange of the building blocks of the different library members and this reaction must meet certain criteria. Several reversible covalent exchanges (Scheme 4) are commonly used, including transamidation,[202–204] ester exchange,[205,206] transimination,[207–209] oxime exchange,[210,211] disulfide exchange,[212,213] hydrazone formation,[214,215] the Diels–Alder reaction,[216] Michael reactions[217], and olefin metathesis.[206,218] Non-covalent reversible interactions, such as hydrogen bonding and metal–ligand coordination, are also employed in the preparation of DCLs.[219–222] Most of these reactions are conducted in aqueous media for biocompatibility. The reversible reaction must occur on a reasonable timescale. Since equilibration and selection typically happen

simultaneously, the reversible reactions need to be compatible with the experimental conditions of the selection process. This includes considering the functional groups on the building blocks and template, as well as factors such as solvent and pH. The reaction conditions used in DCL should be mild to prevent interference with the delicate noncovalent interactions involved in molecular recognition. To avoid undesired cross-reactivity with the functional groups of the building blocks or target molecules, the reactions must be chemoselective.

For proper analysis of the DCL, the building blocks should exhibit comparable reactivity. If mass spectrometry is used for DCL analysis, building blocks should have distinct molecular weights to enable clear differentiation. Additionally, all building blocks must be soluble to prevent precipitation of certain library members, which could bias the data. Dimethyl sulfoxide (DMSO) can be employed as a co-solvent to enhance the solubility of organic compounds. Careful optimization of the co-solvent concentration is necessary to maximize solubility without adversely affecting the target compound.

A DCL should be capable of being “frozen” in the presence of a target molecule, enabling convenient analysis while preserving the library's equilibrium composition. There are several ways to achieve this, including adjusting the pH, removing or inactivating catalysts, or employing irreversible functionalization such as reducing imines to amines.

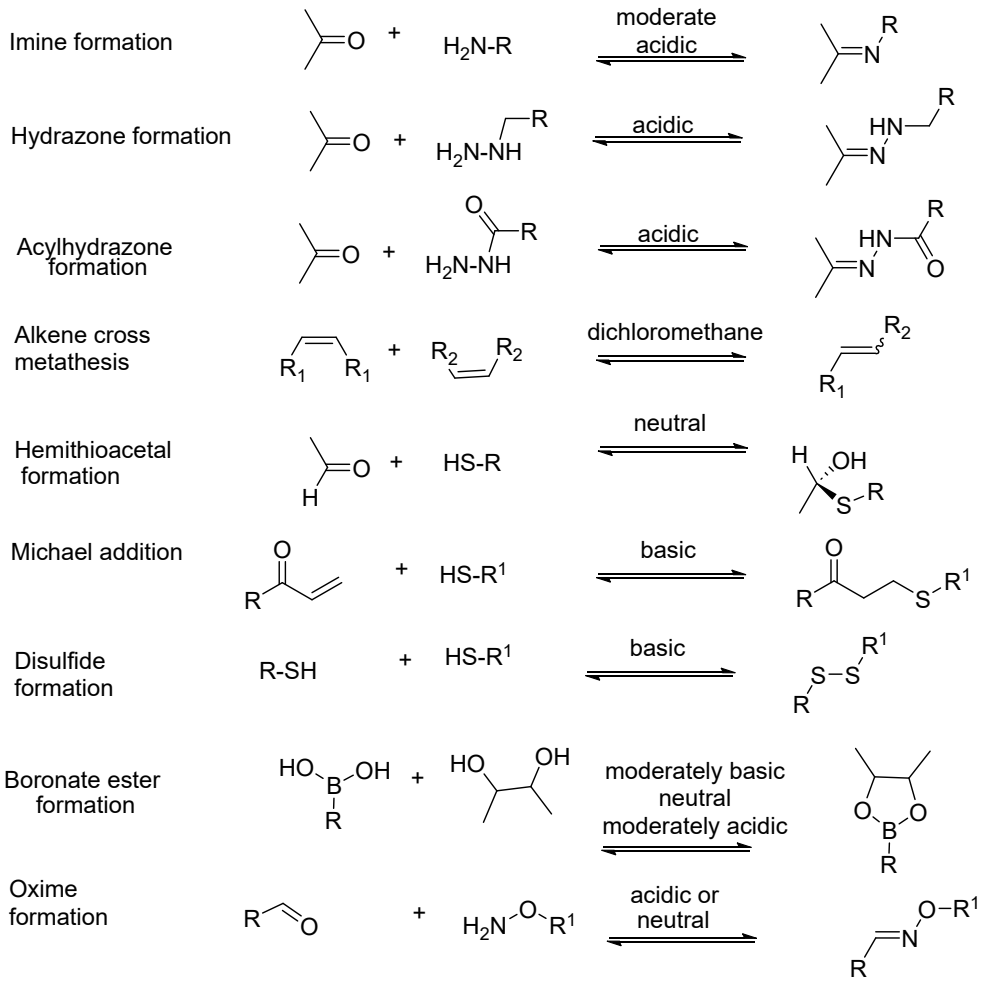

Scheme 4. Reversible reactions used in dynamic combinatorial chemistry.

1.8.2 Dynamic Combinatorial Chemistry for Base-Filling in Nucleic Acid Libraries

Nucleic acids were among the first biological targets explored using DCC.[223] Since then, research in this area has consistently yielded novel and valuable structures for sequence-selective molecular recognition of oligonucleotides. The idea of base-filling was first introduced in 1998 by Hickman, Sreenivasachary, and Lehn[224], although the term itself was coined in 2009 by Heemstra and Liu.[225] Later, the term "side-chain dynamic nucleic acids" (DyNAs) was adopted to describe nucleic acid analogues produced through a similar process.[226] Base filling involves the incorporation of individual bases into an abasic backbone, providing an alternative approach for nonenzymatic templated synthesis of nucleic acids. The presence of a

template strand enables sequence-selective reactions, especially when the coupling reaction is reversible.

An early approach to template-directed oligonucleotide synthesis involved backbone ligation, where two monomeric nucleotides or short oligonucleotides were coupled by connecting their backbone functional groups. This method utilized DNA, RNA or PNA as templates for the ligation process.[227–229] The first application of backbone ligation involved an irreversible reaction that resulted in the formation of a stable phosphodiester bond.[230] Base-filling approach has at least two advantages over the backbone ligation approach. One advantage is that the monomeric nucleobases lack complementary functional groups, which prevents self-reactivity and potentially reduces nontemplated reactions. Another advantage is that the reaction site is in close proximity to the base pairing, which can potentially enhance sequence specificity.

The natural nucleic acid backbones consist of sugars connected by phosphodiester bonds and linked to the base moieties via N-glycosidic linkages. This structure does not allow base filling, as the equilibrium strongly disfavors the formation of the latter in the presence of water.[231–233] On the contrary, the peptide nucleic acid (PNA) backbone is an excellent option, as the peptide bond between the base moiety and the backbone amino function is easily accessible even under aqueous conditions. The resulting product is identical to the corresponding PNA oligonucleotide synthesized using traditional methods, leading to typical high hybridization affinity. However, the irreversibility of the coupling reaction results in modest fidelity, despite a general preference for incorporating the matching Watson–Crick base pairing partner.[225] Besides "native" PNA (Scheme 5A and B), other backbone chemistries adaptable for base filling, such as D-threoninol phosphate (Scheme 5C) and cysteine-rich peptides (Scheme 5D), have been reported,[234,235] incorporating a strong nucleophile in the backbone along with an electrophilic handle on the base moiety.

PNA, an unnatural nucleic acid, has the capacity to hybridize with complementary sequences with high affinity and specificity.[236] Base-filling a PNA backbone has been achieved by both reductive amination and acylation, demonstrating sequence selectivity.[237,238] Base-filling through reductive amination results in the formation of an artificial PNA with a new backbone, known as deoxyPNA, while base-filling of PNA via amine acylation produces native PNA. Both of these base-filling reactions — reductive amination (a reversible reaction) and amine acylation (an irreversible reaction) — demonstrate sequence selectivity. However, reductive amination typically affords higher yields and selectivity compared to amine acylation.

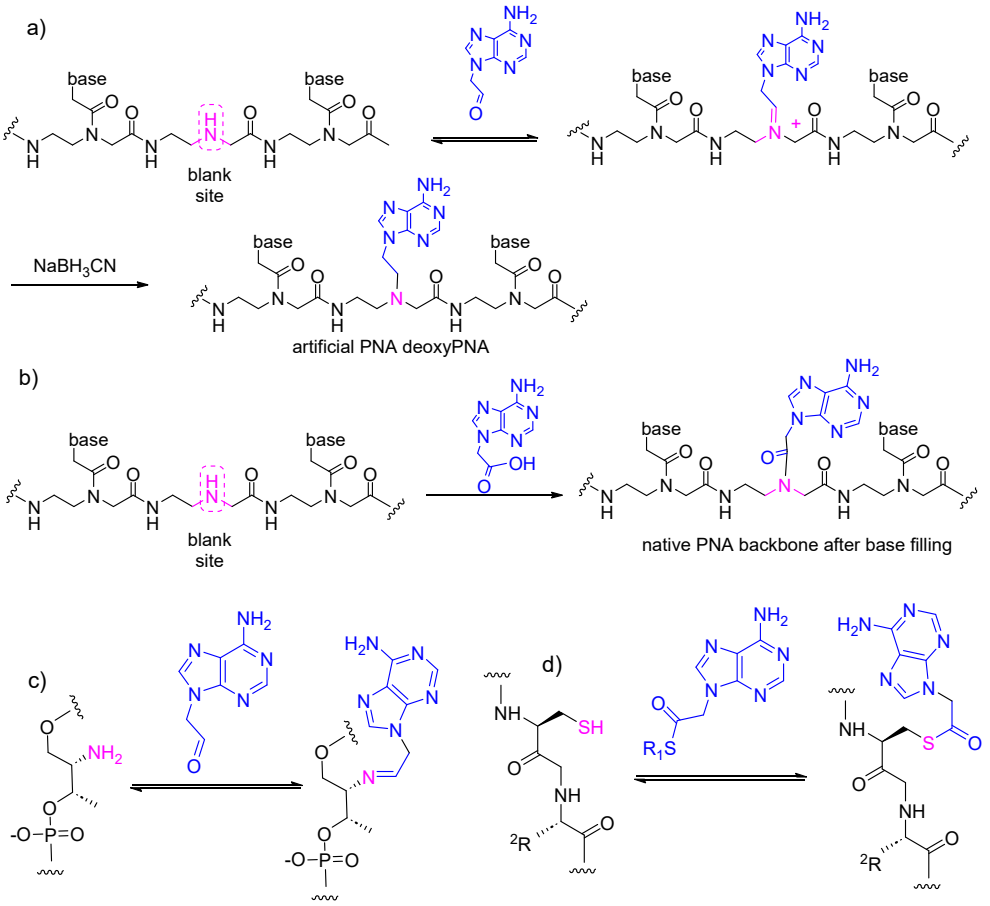

Scheme 5. Base-filling chemistry on a PNA backbone employed by Lui and co-workers.[225] **a**) The base-filling reaction involves the incorporation of nucleobase monomers via reductive amination to produce native PNA **b**) The base-filling reaction involves the incorporation of nucleobase monomers via amine acylation to synthesize deoxyPNA **c**) reductive amination with a D-threoninol backbone; **d**) transthioesterification with a cysteine-containing peptide backbone.

2 Aims of the thesis

Although there are existing technologies for oligonucleotide conjugation, there remains the need for alternative conjugation chemistries that enable straightforward, orthogonal functionalization of modified oligonucleotides. Post-synthetic incorporation of nucleobases or their analogues into oligonucleotides, often called ”base-filling” has emerged as an attractive alternative to conventional stepwise coupling for preparing oligonucleotide libraries that differ by a single residue. Base-filling through reductive amination between nucleobase acetaldehydes and abasic sites within a PNA backbone has been successfully applied for detecting single-nucleotide polymorphisms and circulating microRNAs. Additionally, base filling offers a valuable framework for investigating phenomena such as base pairing, base stacking and ultimately the secondary and tertiary structures of nucleic acids. For such applications, a coupling chemistry more compatible with the sugar-phosphate backbone of natural DNA and RNA would be ideal.

The base-filling reaction should ideally be reversible under conditions that allow Watson-Crick base pairing, facilitating the formation of a DCL. While reductive amination meets this requirement, its reduction step alters the hybridization and geometry of the product. To avoid such complications, a reversible base-filling approach that preserves the hybridization state would be a more suitable alternative. To address the aforementioned needs, this study introduces a novel pH-controlled reversible base filling reaction suitable for DCC, namely the formation of N-methoxy-1,3-oxazinanes and N-methoxy-1,3-oxazolidines through reactions between readily available (2*R*,3*S*)-4-(methoxyamino)butane-1,2,3-triol-modified oligonucleotides and aldehydes. The aims of the thesis can be summarized as follows:

I Developing a robust synthesis strategy for oligonucleotides incorporating residues that allow reversible pH-controlled base-filling.

II Elucidating the factors affecting the rate and equilibrium of the base-filling reactions.

III Verifying the selectivity of the base-filling reactions in terms of Watson—Crick base pairing.

3 Results and Discussion

3.1 Synthesis of aldehydes

The syntheses of the four canonical nucleobase analogues have been described in the literature.[239,240] For control experiments, 2-(2-methylbenzimidazol-1-yl)acetaldehyde (Scheme 6) was synthesized using the same method as with the canonical nucleobases. This compound, which acts as a purine base for base stacking effects, contains no hydrogen bond donors or acceptors. 2-methylbenzimidazole **1** was thus alkylated at the N3 position with bromoacetaldehyde diethyl acetal to yield compound **2**, which was hydrolyzed by aqueous HCl to afford 2-(2-methylbenzimidazol-1-yl)acetaldehyde **3**.

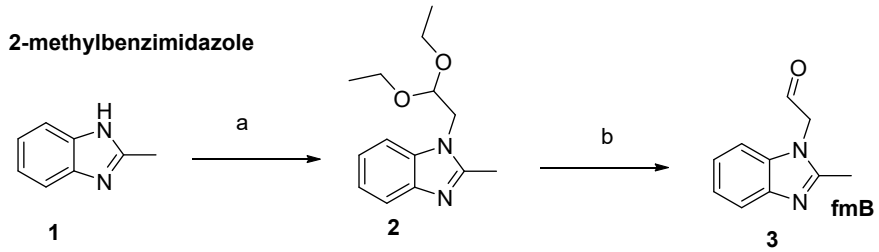

Scheme 6. 2-(2-methylbenzimidazol-1-yl) acetaldehyde. Reagents and conditions: a) bromoacetaldehyde diethyl acetal, Cs_2CO_3, DMF, 90 °C, 90 min; b) HCl, H_2O, 90 °C, 60 min.

3.2 Synthesis of (2R,3S)-4-(methoxyamino)butane-1,2,3-triol (MABT)

Preparation of (2*R*,3*S*)-4-(methoxyamino)butane-1,2,3-triol (**8**) is outlined in Scheme 7. Oxidation of methyl 4,6-*O*-benzylidene-α-D-glucopyranoside (**4**) yielded (4*R*)-5-((*S*)-1-methoxy-2-oxoethoxy)-2-phenyl-1,3-dioxane-4-carbaldehyde (**5**). Oximation of compound **5** gave a mixture of geometric isomers, the major one being (2S,E)-2-methoxy-2-(((4S)-4-((E)-(methoxyimino)methyl)-2-phenyl-1,3-dioxan-5-yl)oxy)acetaldehyde *O*-methyl oxime (**6**). Reduction of compound **6** afforded *N*-((2S)-2-methoxy-2-(((4S)-4-((methoxyamino)methyl)-2-phenyl-1,3-dioxan-5-yl)oxy)ethyl)-*O*-methylhydroxylamine (**7**). Subsequently, acid-catalyzed

hydrolysis of **7** removed acetal protections, resulting in (2R,3S)-4-(methoxyamino)butane-1,2,3-triol (**8**).

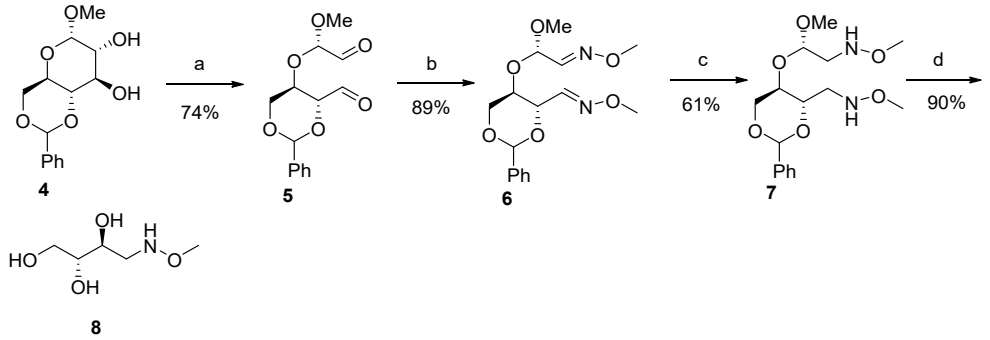

Scheme 7. Synthesis of the protected (2*R*,3*S*)-4-(methoxyamino)butane-1,2,3-triol. Reagents and conditions: a) $NaIO_4$, MeOH, H_2O, 25 °C, 20 h; b) $MeONH_3Cl$, pyridine, 80 °C, 16 h; c) $NaCNBH_3$, AcOH, CH_2Cl_2, MeOH, 25 °C, 16 h; d) HCl, 1,3-propanedithiol, H_2O, 40 °C, 16 h.

3.2.1 Synthesis of Fmoc-protected MABT phosphoramidite

The synthesis of Fmoc-protected MABT phosphoramidite **14** was performed following the procedure outlined in Scheme 8. Initially, the methoxyamino group in compound **8** was protected with a 9-fluorenylmethoxycarbonyl (Fmoc) group, resulting in compound **9**. The primary alcohol in compound **9** was then dimethoxytritylated to yield compound **10**. Next, the base-labile Fmoc group on compound **10** was removed, producing compound **11**. Compound **11** subsequently underwent silylation to yield compound **12**, followed by the reintroduction of the Fmoc group to produce compound **13**. Finally, compound **10** was phosphitylated, generating the desired phosphoramidite building block **14**.

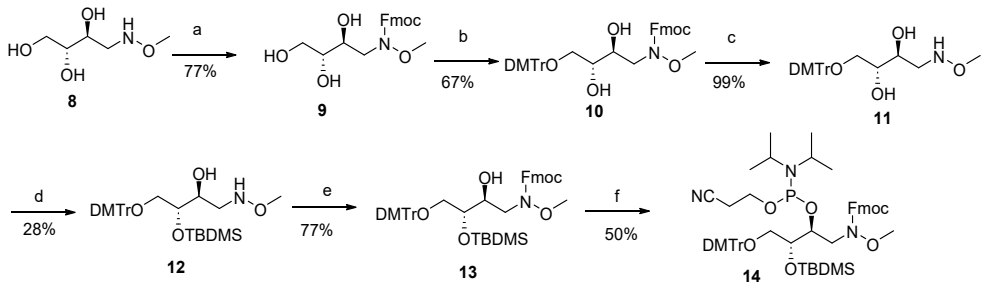

Scheme 8. Synthesis of the F-moc protected phosphoramidite building block **1**. a) FmocCl, K_2CO_3, 1,4-dioxane, H_2O, 25 °C, 16 h; b) DMTrCl, CH_2Cl_2, pyridine, N_2 atmosphere, 25 °C, 16 h; c) Et_2NH, CH_2Cl_2, 25 °C, 45 min; d) TBDMSCl, imidazole, DMF, 25 °C, 16 h; e) FmocCl, K_2CO_3, 1,4-dioxane, H_2O, 25 °C, 16 h; f) 2-cyanoethyl-*N*,*N*-diisopropylaminophosphoramidite, Et_3N, CH_2Cl_2, N_2 atmosphere, 25 °C, 45 min.

3.2.2 Synthesis of 4-(benzoyloxy)benzylidene-protected MABT phosphoramidite

The synthesis of the 4-(benzoyloxy)benzylidene-protected (2*R*,3*S*)-4-(methoxyamino)butane-1,2,3-triol phosphoramidite building block **17** is outlined in Scheme 9. The process began with the reaction of (2R,3S)-4-(methoxyamino)butane-1,2,3-triol with 4-(benzoyloxy)benzaldehyde in the presence of acetic acid to afford compound **15**. The primary hydroxy group of compound **15** was then protected as a dimethoxytrityl ether to form intermediate **16**. Finally, the remaining secondary hydroxy group was phosphitylated using standard methods to yield the phosphoramidite building block **17**.

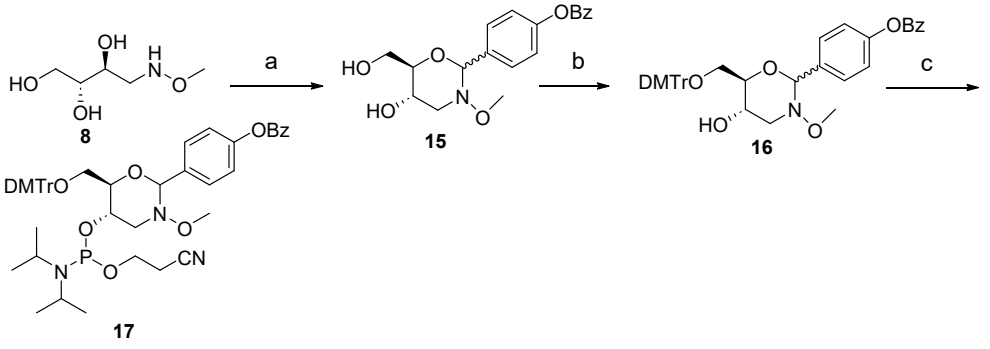

Scheme 9. Synthesis of the 4-(benzoyloxy)benzylidene protected (2*R*,3*S*)-4-(methoxyamino)butane-1,2,3-triol phosphoramidite building block **17**. Reagents and conditions: a) 4-benzoyloxybenzaldehyde, AcOH, 1,4-dioxane, 50 °C, 16 h; b) DMTrCl, CH_2Cl_2, pyridine, N_2 atmosphere, 25 °C, 16 h; c) 2-cyanoethyl-*N*,*N*-diisopropylchlorophosphoramidite, Et_3N, CH_2Cl_2, N_2 atmosphere, 25 °C, 1 h.

3.2.3 Synthesis of para-nitrobenzylidene-protected MABT phosphoramidites

The synthesis of the para-nitrobenzylidene-protected phosphoramidites **20** and **23** is illustrated in Scheme 10. Initially, (2R,3S)-4-(methoxyamino)butane-1,2,3-triol (**8**) was reacted with 4-nitrobenzaldehyde under acidic conditions to produce compound **18**. The primary hydroxy group of compound **18** was 4,4′-dimethoxytritylated resulting in compound **19**. Finally, the secondary hydroxy group of compound **19** was phosphitylated using standard procedures to obtain phosphoramidite **20**. Phosphoramidite **23** was synthesized following a similar approach, but with an extended reaction time between (2R,3S)-4-(methoxyamino)butane-1,2,3-triol and 4-nitrobenzaldehyde under acidic conditions. This prolonged reaction favored the formation of the thermodynamically preferred six-membered oxazinane ring, yielding compound **21**. The primary hydroxyl group of compound **21** was subsequently protected by dimethoxytritylation to form compound **22**, which was then phosphitylated via conventional methods to afford phosphoramidite **23**.

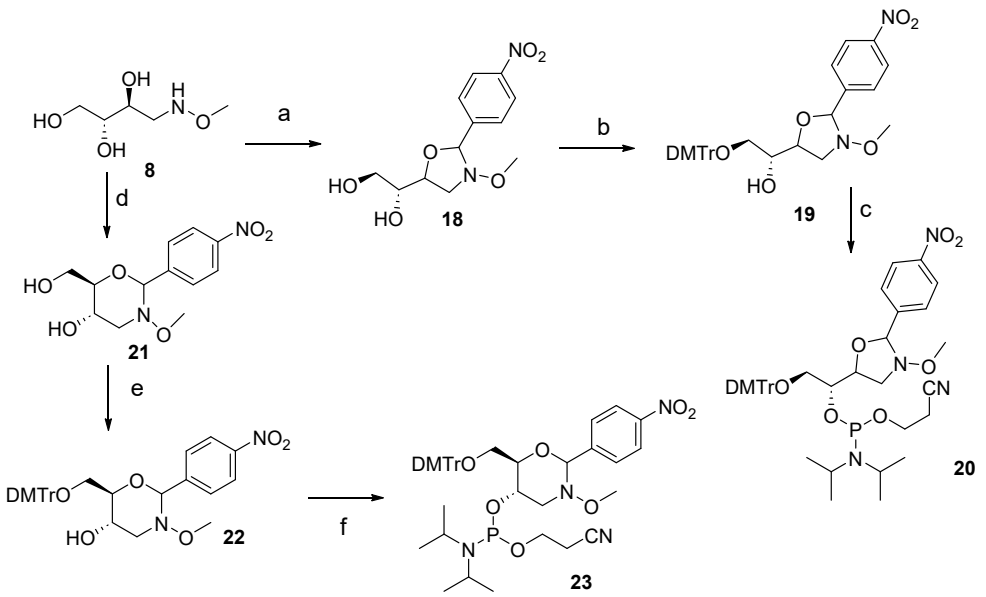

Scheme 10. Synthesis of the protected (2*R*,3*S*)-4-(methoxyamino)butane-1,2,3-triol phosphoramidite building block **20** and **23**. Reagents and conditions: a) 4-nitrobenzaldehyde, AcOH, 50 °C, 3 h; b) DMTrCl, CH_2Cl_2, pyridine, N_2 atmosphere, 25 °C, 14 h; c) 2-cyanoethyl-*N*,*N*-diisopropylaminophosphoramidite, Et_3N, CH_2Cl_2, N_2 atmosphere, 25 °C, 1 h. d) 4-nitrobenzaldehyde, AcOH, 50 °C, 15 h; e) DMTrCl, CH_2Cl_2, pyridine, N_2 atmosphere, 25 °C, 14 h; f) 2-cyanoethyl-*N*,*N*-diisopropylaminophosphoramidite, Et_3N, CH_2Cl_2, N_2 atmosphere, 25 °C, 1 h.

3.3 Oligonucleotides synthesis

Oligonucleotide syntheses were performed on an ÄKTA Oligopilot Plus 10 DNA/RNA synthesizer at a 1-2 µmol scale using CPG solid support, following the conventional phosphoramidite strategy. **Table 1** summarizes the sequences and structural modifications of synthesized oligonucleotides and commercial products employed in this study. Commercially sourced oligonucleotides **ON11a, ON11c, ON11g, ON11t, ON12a, ON12c, ON12g** and **ON12t** were used without further modification. Modified oligonucleotides were synthesized using different phosphoramidite building blocks. Phosphoramidite **14** was utilized for the synthesis of DNA-MOANA oligonucleotide **ON1** while phosphoramidite **17** was employed to synthesize DNA-MOANA oligonucleotides **ON2a**, **ON2c**, **ON2g**, **ON2t**, and **ON2s**.[241]. The coupling yield of phosphoramidite **14** was only approximately 64% despite a prolonged coupling time of 15 min, while the other couplings proceeded with normal (>99%) efficiency. The coupling yield of phosphoramidite **17** was 99%. Building blocks **20** and **23** were employed to introduce a single MOGNA or MOANA residue into oligonucleotides **ON3**, **ON4a**, **ON4c**, **ON4g**, **ON4t**, **ON4s**, **ON5**, **ON6a**, **ON6c**, **ON6g**, **ON6u**, **ON6s**, **ON7**, **ON8a**, **ON8c**, **ON8g**, **ON8u**, **ON8s, ON9** and **ON10**. MOANA and MOGNA phosphoramidite building blocks **20** and **23** showed coupling yields between 77% and 99% based on trityl response measurements. After synthesis, oligonucleotides were cleaved from the solid support and deprotected by incubation in 25% aqueous ammonia at 55 °C for 16 hours.

Table 1. Sequences of the oligonucleotides used in this study. The variable residues (base-filling scaffolds and nucleotides opposite to them) are underlined.

Oligonucleotide	Sequence (5´-3´)[a]
ON1	5´-CGA GCX CTG GC-3´
ON2a	5´-GCC AGA GCT CGT TTT CGA GCX CTG GC-3´
ON2c	5´-GCC AGC GCT CGT TTT CGA GCX CTG GC-3´
ON2g	5´-GCC AGG GCT CGT TTT CGA GCX CTG GC3´
ON2t	5´-GCC AGT GCT CGT TTT CGA GCX CTG GC3´
ON2s	5´-GCC AGS GCT CGT TTT CGA GCX CTG GC3´
ON3	5´-CGA GCY CTG GC-3´
ON4a	5´-GCC AGA GCT CGT TTT CGA GCY CTG GC3´
ON4c	5´-GCC AGC GCT CGT TTT CGA GCY CTG GC3´
ON4g	5´-GCC AGG GCT CGT TTT CGA GCY CTG GC3´
ON4t	5´-GCC AGT GCT CGT TTT CGA GCY CTG GC3´
ON4s	5´-GCC AGS GCT CGT TTT CGA GCY CTG GC3´
ON5	5´-cga gcX cug gc-3´
ON6a	5´-gcc aga gcu cgu uuu cga gcX cug gc-3´
ON6c	5´-gcc agc gcu cgu uuu cga gcX cug gc-3´
ON6g	5´-gcc agg gcu cgu uuu cga gcX cug gc-3´
ON6u	5´-gcc agu gcu cgu uuu cga gcX cug gc-3´
ON6s	5´-gcc ags gcu cgu uuu cga gcX cug gc-3´
ON7	5´-cga gcY cug gc-3´
ON8a	5´-gcc aga gcu cgu uuu cga gcY cug gc-3´
ON8c	5´-gcc agc gcu cgu uuu cga gcY cug gc-3´
ON8g	5´-gcc agg gcu cgu uuu cga gcY cug gc-3´
ON8u	5´-gcc agu gcu cgu uuu cga gcY cug gc-3´
ON8s	5´-gcc ags gcu cgu uuu cga gcY cug gc-3´
ON9	5´-TTT TTT TTT TTT TTT XT-3´
ON10	5´-TTT TTT TTT TTT TTT YT-3´
ON11a	5´-GAT TTT TTT TTT TTT TTG C-3´
ON11c	5´-GCT TTT TTT TTT TTT TTG C-3´
ON11g	5´-GGT TTT TTT TTT TTT TTG C-3´
ON11t	5´-GTT TTT TTT TTT TTT TTG C-3´
ON12a	5´-GCA AAA AAA AAA AAA AAA C-3´
ON12c	5´-GCA AAA AAA AAA AAA AAC C-3´
ON12g	5´-GCA AAA AAA AAA AAA AAG C-3´
ON12t	5´-GCA AAA AAA AAA AAA AAT C-3´

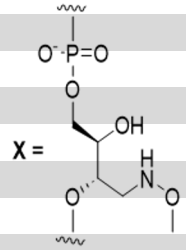

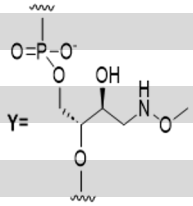

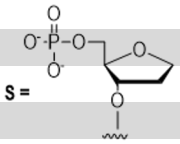

[a] Uppercase letters refer to DNA and lowercase letters to 2´-O-methyl-RNA nucleotides, “X” to the MOANA residue, “Y” to the MOGNA residue and “S” to the abasic 2-(hydroxymethyl)tetrahydrofuran-3-ol spacer.

3.4 Formation of N-methoxy-1,3-oxazinane oligonucleotides

The formation of *N*-methoxy-1,3-oxazinane residues within oligonucleotides was initially examined by reacting **ON1** with an excess of various aromatic (e.g., benzaldehyde, 3-hydroxybenzaldehyde, 3-methoxybenzaldehyde, 3-cyanobenzaldehyde, 3-nitrobenzaldehyde, isophthalaldehyde, imidazole-2-carbaldehyde, and quinoline-2-carbaldehyde) as well as aliphatic (e.g., butyraldehyde and benzyloxyacetaldehyde) aldehydes. Each reaction was conducted separately, allowing **ON1** to react with a single aldehyde under mildly acidic conditions (pH 5.0) at 55°C overnight. After the reaction, the mixture was quenched by adjusting the pH to 7.0. The aqueous solution was then washed with dichloromethane and analysed by reverse-phase high-performance liquid chromatography (RP-HPLC). A representative chromatogram is shown in Figure 8. As anticipated, the reaction of **ON1** with 3-nitrobenzaldehyde led to the formation of an *N*-methoxy-1,3-oxazinane-functionalized oligonucleotide, which eluted more slowly. Table 2 provides a summary of the retention times, yields, and both the calculated and observed *m*/*z* values of the products. Mass spectrometric analysis of confirmed the formation of *N*-methoxy-1,3-oxazinanes in each case. The yields ranged from 24% to 82%, the lowest ones being obtained with relatively volatile aldehydes, such as benzaldehyde (24%) and butyraldehyde (33%). The reaction was shown to be reversible under mildly acidic conditions (pH 5.0) and stable at pH 7.0.

Table 2. RP-HPLC retention times, yields and calculated and observed *m*/*z* values of the products of the reactions of the oligonucleotide scaffold **ON1** with various aldehydes.

Aldehyde	t_R/min[a]	yield/%[b]	cald.m/z	obs.m/z[c]
benzaldehyde	17.7	24	1663.8	1663.8
3-hydroxybenzaldehyde	15.8	78	1671.8	1671.8
3-methoxybenzaldehyde	17.4	55	1678.8	1678.8
3-cyanobenzaldehyde	17.1	63	1676.3	1676.3
3-nitrobenzaldehyde	17.8	82	1686.3	1686.3
isophthaladehyde	16.0	71	1677.8	1677.8
imidazole-2-carbaldehyde	11.3	80	1658.8	1658.8
quinoline-2-carbaldehyde	12.7	53	1689.3	1689.3
butyraldehyde	15.9	33	1646.8	1646.8
benzyloxyacetaldehyde	16.6	82	1685.8	1685.8

[a] For HPLC conditions, see Figure 8.
[b] Estimated based on relative peak areas in HPLC.
[c] Bruker Daltonics micrOTOF-Q, $[M - 2H]^{2-}$

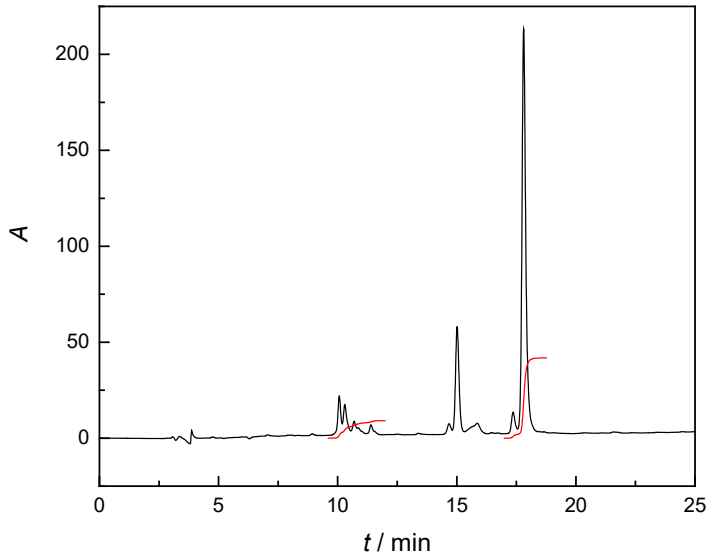

Figure 8. A) RP-HPLC trace of the product mixture of the reaction of the oligonucleotide scaffold **ON1** with 3-nitrobenzaldehyde (method A); Hypersil ODS C18 column (250 × 4.6 mm, 5 µm); detection wavelength = 260 nm; flow rate = 1.0 mL min-1; linear gradient (8—23% over 25 min) of acetonitrile in 50 mM aqueous triethylammonium acetate (pH = 7.0).

3.5 Thermal stability of the modified duplexes and triplexes

Incorporating a modified building block into the DNA/RNA sequence has the tendency of impacting the hybridization affinity. The formation and hydrolysis of *N*-methoxy-1,3-oxazinanes and *N*-methoxy-1,3-oxazolidines are acid-catalyzed processes that proceed relatively slowly at neutral pH. However, excessively acidic conditions could disrupt the hybridization of oligonucleotide scaffolds into the desired hairpin or triplex structures. To ensure the stability of the hairpins and triplexes under conditions where the incorporation and dissociation of nucleobase analogs occur at a reasonable rate, their UV melting profiles were measured under the slightly acidic conditions (pH = 5.5) of the DCC experiments. The UV melting experiments were conducted for various hairpin structures (**Figure 10**), including DNA–MOANA (**ON2a, ON2c, ON2g, ON2t, and ON2s**), DNA–MOGNA (**ON4a, ON4c, ON4g, ON4t,** and **ON4s**), 2'-OMe-RNA–MOANA (**ON6a**, **ON6c**, **ON6g**, **ON6u** and **ON6s**) and 2'-OMe-RNA–MOGNA (**ON8a**, **ON8c**, **ON8g**, **ON8u** and **ON8s**) hairpins. For DNA–MOANA hairpins (**ON2a, ON2c, ON2g, ON2t,** and **ON2s**), UV melting temperatures were measured over a temperature range of 10–90 °C in a 100 mM triethylammonium acetate buffer (pH 5.5). For DNA–MOGNA hairpins (**ON4a, ON4c, ON4g, ON4t,** and **ON4s**), as well as 2'-OMe-RNA–

MOANA and 2'-OMe-RNA–MOGNA hairpins (**ON6a, ON6c, ON6g, ON6u, ON6s, ON8a, ON8c, ON8g, ON8u,** and **ON8s**), UV melting temperatures were determined in a 20 mM cacodylate buffer (pH 5.5) with an ionic strength of 0.10 M, adjusted with sodium perchlorate. The melting temperatures for the DNA—MOANA hairpins ranged from 54 to 57 °C, whereas the DNA—MOGNA hairpins exhibited significantly higher melting temperatures, ranging from 62 to 68 °C (Figure 9), although there is only a slight structural difference between them. The 2′-OMe-RNA—MOANA and 2′-OMe-RNA—MOGNA hairpins exhibited even higher melting temperatures, ranging from 74 to 82 °C. The high melting temperature of 2′-OMe-RNA is attributed to its 2'-O-methyl group on the ribose sugar, which increases the rigidity of the RNA strand. This rigidity enhances base stacking interactions, resulting in a more stable double helix.

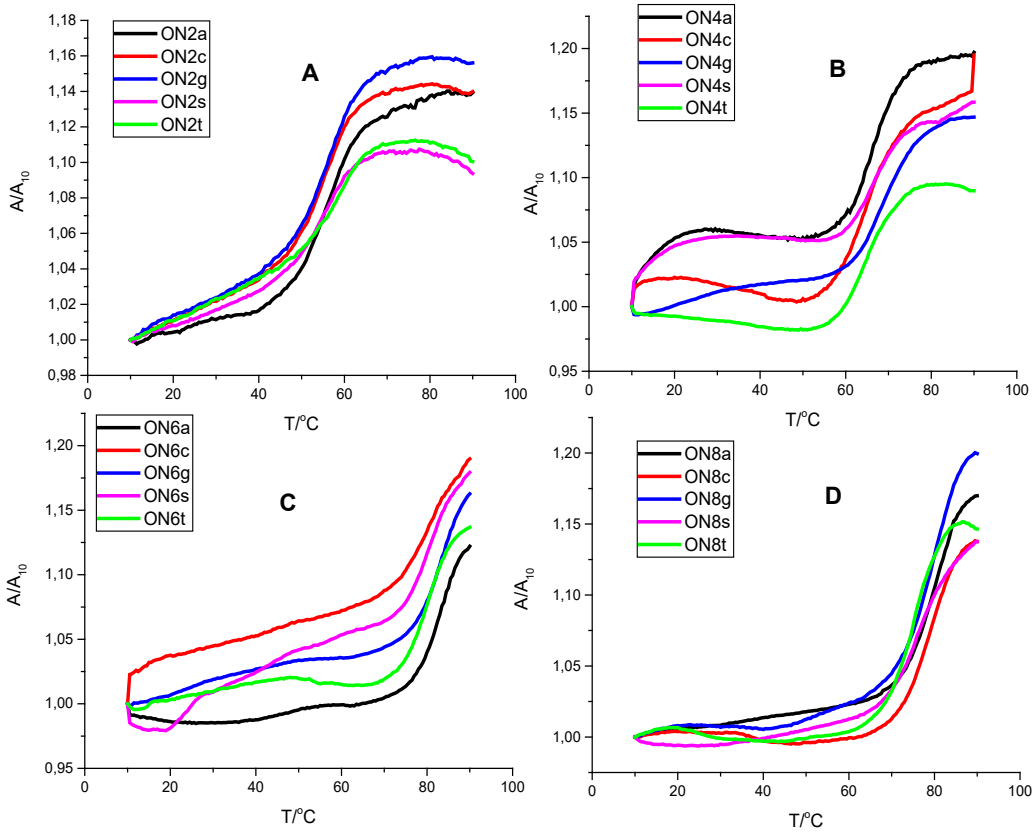

Figure 9. UV melting curves obtained for 1.0 μM solutions of hairpins A) **ON2a, ON2c, ON2g, ON2t, and ON2s** in a 100 mM triethylammonium acetate buffer at pH 5.5, B) **ON4a, ON4c, ON4g, ON4t, ON4s,** C) **ON6a, ON6c, ON6g, ON6t, ON6s,** D) **ON8a, ON8c, ON8g, ON8t,** and **ON8s**, using a 20 mM cacodylate buffer at pH 5.5 with an ionic strength of 0.10 M ($NaClO_4$).

Similar experiments were performed under the same conditions for the triplexes **ON11t•ON12a*ON9**, **ON11g•ON12c*ON9**, **ON11c•ON12g*ON9** and **ON11a•ON12t*ON9** and **ON11t•ON12a*ON10**, **ON11g•ON12c*ON10**, **ON11c•ON12g*ON10** and **ON11a•ON12t*ON10.** The melting curves of the triplexes displayed a biphasic pattern as shown in **Figure 10**. The higher melting temperature, associated with the unwinding of the Watson-Crick double helix, was remarkably consistent across all triplexes, averaging around 42 °C. In contrast, the lower melting temperature, which corresponds to the dissociation of the triplex-forming oligonucleotide **ON9** or **ON10** from the double helix, exhibited much greater variation, ranging from 21 to 31 °C. This means that in some triplexes, significant Hoogsteen melting could occur even at room temperature (23 °C). However, this temperature was still selected for the DCC experiments, as lowering it further to minimize Hoogsteen melting would have made equilibration of the DCL impractically slow.

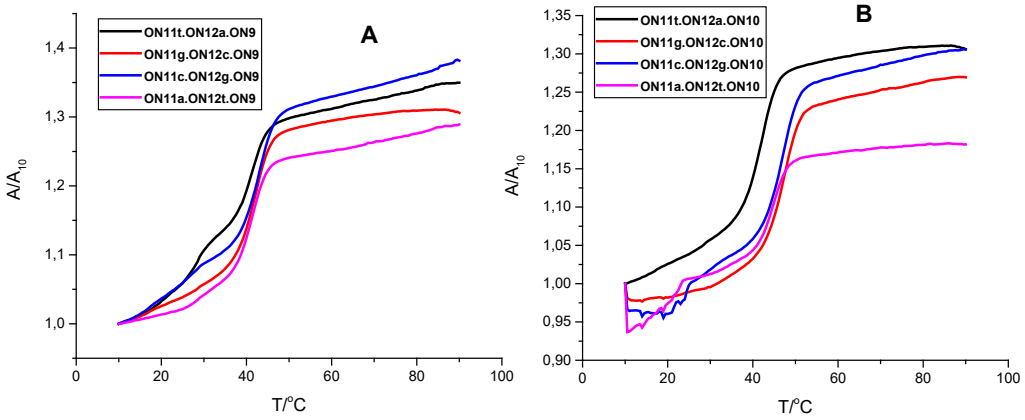

Figure 10. UV melting profiles of 1.0 μM triplex A) **ON11t•ON12a*ON9** (black), **ON11g•ON12c*ON9** (red), **ON11c•ON12g*ON9** (blue), **ON11a•ON12t*ON9** (pink), B) **ON11t•ON12a*ON10** (black), **ON11g•ON12c*ON10** (red), **ON11c•ON12g*ON10** (blue) and **ON11a•ON12t*ON10** (pink); pH = 5.5 (20 mM cacodylate buffer); *I*(NaClO4) = 0.10 M.

3.6 Kinetics of N-methoxy-1,3-oxazinane and -oxazolidine formation and decomposition

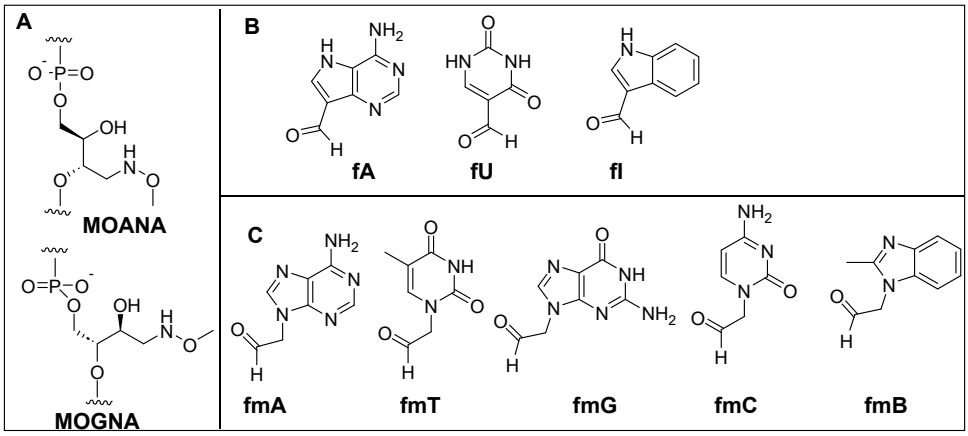

Figure 11. Starting materials for the DCC experiments A) Modified oligonucleotides bearing a 4-methoxyaminobutane-1,2,3-triol residue B) 9-formyl-9-deazaadenine (**fA**) and 5-formyluracil (**fU**), indole-3-carbaldehyde (**fI**) C) formylmethyl derivatives of the canonical nucleobases (**fmA, fmC, fmG** and **fmT**) and2-(2-methylbenzimidazol-1-yl)acetaldehyde (**fmB**).

The kinetics of *N*-methoxy-1,3-oxazinane decomposition were determined using selected hairpin oligonucleotides (**ON2a, ON2c ON2g ON2s and ON2t**) and aldehydes, specifically 9-formyl-9-deazaadenine (**fA**), 5-formyluracil (**fU**) and indole-3-carbaldehyde (**fI**) shown in Figure 11B. **fU** and **fI** are commercially available aldehydes and the synthesis of **fA** has been reported.[242] Oligonucleotide-aldehyde mixtures were incubated for several days in a buffered aqueous solution (0.1 M triethylammonium acetate, pH 5.5, and at a high concentration (500 μM) to ensure incorporation of a significant fraction of the aldehyde into the oligonucleotide. The reaction mixtures were then diluted to a concentration of 1.0 μM, where nearly complete dissociation was expected, and their compositions were monitored over time using RP-HPLC. All oligonucleotide components eluted as a single broad peak, so quantification was based on the relative peak area of the free aldehyde and the formation of *N*-methoxy-1,3-oxazinane conjugates was confirmed by UPLC-MS. Notably, in each case, only a single aldehyde molecule was incorporated, excluding the possibility of non-specific imine formation with the exocyclic amino groups of the nucleobases. Time-dependent increases in aldehyde concentration were observed and the reactions strictly followed first-order kinetics. The first-order rate constants for dissociation were determined by non-linear least-squares fitting of the experimental data to **Equation 1**.

$$[\text{aldehyde}]_t = ([\text{aldehyde}]_{eq} - [\text{aldehyde}]_0)\,(1 - e^{-kt}) + [\text{aldehyde}]_0 \quad (1)$$

In this equation, $[\text{aldehyde}]_0$, $[\text{aldehyde}]_t$ and $[\text{aldehyde}]_{eq}$ represent the concentrations of free aldehyde at the start, at time t, and at equilibrium, respectively, with *k* as the observed first-order rate constant.

Table 3. Observed first-order rate constants for the release of aldehydes **fA**, **fU** and **fI** from hairpin oligonucleotides **ON2a**, **ON2c**, **ON2g**, **ON2t** and **ON2s**; *T* = 23 °C; pH = 5.5 (100 mM triethylammonium acetate buffer).

Oligonucleotide	***k*(fA)**/10^{-5} s^{-1}	***k*(fU)**/10^{-5} s^{-1}	***k*(fI)**/10^{-5} s^{-1}
ON2a	3.4 ± 0.8	2.5 ± 0.6	2 ± 1
ON2c	9 ± 1	1.4 ± 0.1	1.3 ± 0.5
ON2g	4.6 ± 0.2	0.4 ± 0.3	2 ± 1
ON2t	4 ± 2	1.5 ± 0.5	0.6 ± 0.4
ON2s	7 ± 4	1.1 ± 0.6	4.0 ± 0.9

The observed reaction rates are summarized in **Table 3**. The rate constants for the incorporation of aldehydes into oligonucleotides varied between 3.4 and 9 × 10^{-5} s^{-1} for **fA**, 0.4 and 2.5 × 10^{-5} s^{-1} for **fU** and 0.6 and 4 × 10^{-5} s^{-1} for **fI**. The decomposition of **ON2c-fA** exhibited the highest reaction rate. The dissociation rate was primarily influenced by the structural differences of the aldehydes, following a general trend of **fU** < **fI** < **fA**. Based on the observed rate constants, the optimal equilibration time for the DCC analysis was determined to be 48 h for **fA** and 120 h for both **fU** and **fI**.

The kinetics of base-filling were determined by analyzing the composition of the reaction mixtures at specific time intervals using UPLC-TOF-MS. Hairpin oligonucleotides **ON2t, ON4t, ON6u,** and **ON8u** and the aldehyde **fmA** were selected for this study. Each of the oligonucleotides (1.0 μM) and the aldehyde (2.0 μM) were incubated for several days in a 20 mM cacodylate buffer (0.1 M $NaClO_4$, pH 5.5) at 23 °C. Figure 12 illustrates the reaction rates for the formation of N-methoxy-1,3-oxazinane and N-methoxy-1,3-oxazolidine, which range from 0.5×10^5 to 1.75×10^5 s^{-1}. Among the reactions, **ON4t + fmA** exhibited the highest reaction rate (1.75×10^5 s^{-1}), while **ON8U + fmA** had the lowest (0.5×10^5 s^{-1}). The reaction rates for **ON2t + fmA** and **ON6U + fmA** were similar, approximately (1.5−1.6×10^5 s^{-1}). In each case, the first-order disappearance of the starting material was observed, accompanied by the formation of the **fmA** adduct with half-lives ranging from 9 to 32 h and no clear dependence on the backbone structure. A reaction time of 120 h, equivalent to 4–13 half-lives, was considered sufficient for the DCC reactions.

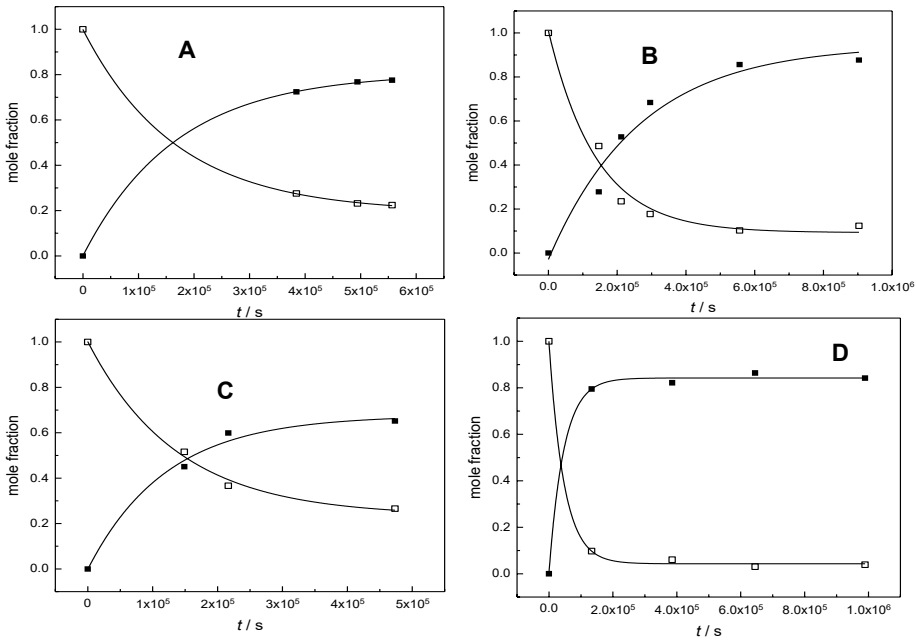

Figure 12. Time-dependent mole fraction of oligonucleotide **ON2t** (A), **ON4t** (B), **ON6u, and ON8u** (□) and its 9- formylmethyladenine adduct (■); pH = 5.5 (20 mM cacodylate buffer); *I*($NaClO_4$) = 0.10; [oligonucleotides] = 1.0 μM; [aldehydes] = 2.0 μM.

3.7 Equilibria of N-methoxy-1,3-oxazinane formation

The equilibrium constants for the formation of *N*-methoxy-1,3-oxazinanes were determined to evaluate the stability of the conjugates obtained by incorporating each aldehyde (**fA, fU,** and **fI**) into the hairpin oligonucleotides (**ON2a**, **ON2c**, **ON2g**, **ON2s** and **ON2t**). A series of equimolar (1–500 μM) mixtures of each aldehyde and oligonucleotide were first prepared and incubated in a buffered aqueous solution (0.1 M triethylammonium acetate, pH 5.5) at 23 °C for an appropriate time period (48 h for **fA** and 120 h for **fU** and **fI**). The mixtures were then analyzed by RP-HPLC. As the total aldehyde and oligonucleotide concentrations of all mixtures were equimolar, decrease in the concentration of the free aldehyde translates to increase in the concentration of the aldehyde incorporated to the hairpin oligonucleotide. The stability constants were determined by non-linear least-squares fitting of **Equation 2** to the experimental data.

$$A(\text{aldehyde})_c = A(\text{aldehyde})_0 + (A(\text{aldehyde})_\infty - A(\text{aldehyde})_0)\left(1 + \frac{1-\sqrt{4Kc+1}}{2Kc}\right) \quad (2)$$

$A(\text{aldehyde})_o$, $A(\text{aldehyde})_c$ and $A(\text{aldehyde})_\infty$ are relative peak areas of the free aldehyde at zero, c and infinite concentration of the aldehyde and the oligonucleotide, respectively. By definition, the concentration of the free aldehyde

is equal to the total aldehyde concentration at $c = 0$ (i.e., infinite dilution) and approaches zero as $c \rightarrow \infty$. However, in practice, more reliable results were obtained by fitting these parameters in the equation above. K represents the stability constant of the oligonucleotide-aldehyde conjugate and c the total concentration of both the oligonucleotide and the aldehyde.

Table 4. Stability constants for the covalent conjugates of aldehydes **fA**, **fU** and **fI** with hairpin oligonucleotides **ON2a**, **ON2c**, **ON2g**, **ON2t** and **ON2s**; T = 23 °C; pH = 5.5 (100 mM triethylammonium acetate buffer).

Oligonucleotide	***K*(fA)**/10^3 M^{-1}	***K*(fU)**/10^3 M^{-1}	***K*(fI)**/10^3 M^{-1}
ON2a	20 ± 10	13 ± 6	12 ± 5
ON2c	200 ± 100	9 ± 5	3 ± 2
ON2g	300 ± 200	30 ± 30	50 ± 40
ON2t	700 ± 400	12 ± 10	5 ± 3
ON2s	3 ± 2	8 ± 5	8 ± 8

The stability constants shown in **Table 4** for the covalent conjugates of aldehydes **fA**, **fU** and **fI** with hairpin oligonucleotides **ON2a**, **ON2c**, **ON2g**, **ON2t** and **ON2s** were between 3 and 700 × 10^3 M^{-1} for **fA**, 8 and 30 × 10^3 M^{-1} for **fU** and 3 and 50 × 10^3 M^{-1} for **fI**. The adenine analogue **fA** showed 1–2 orders of magnitude higher affinity for hairpin oligonucleotides **ON2c**, **ON2g**, and **ON2t** compared to **fU** and **fI**. In contrast, the affinities for **ON2a** and **ON2s** were lower, comparable to those of **fU** and **fI** . Notably, the highest stability constant was observed when **fA** paired with thymine, which is consistent with Watson-Crick base pairing. The relatively high affinity of **ON2c** and **ON2g** suggests the presence of hydrogen bonding interactions with both cytosine and guanine. The importance of hydrogen bonding in determining affinity is also evident from the low incorporation efficiency of **fA** into **ON2s**, an oligonucleotide containing an abasic site opposite **fA**. The affinity of **ON2a** was intermediate between that of **ON2s** and **ON2c**, likely due to weak mismatched base pairing. With the exception of **fA** incorporation into hairpin **ON2s**, nearly all conjugates formed through the incorporation of **fU** were less stable than those formed with **fA**. In summary, **fA**, with its large stacking surface and array of hydrogen bond donors and acceptors, showed the highest affinity and selectivity, following Watson-Crick base pairing rules. In contrast, 5-formyluracil (**fU**) and indole-3-carbaldehyde (**fI**), which lacked either stacking or hydrogen bonding capabilities, demonstrated significantly lower affinity and selectivity.

3.8 DCC experiment for base pairing selectivity

The efficiency and selectivity of base-filling MOANA or MOGNA residues inside a double helix were examined by incubating 1.0 μM of each hairpin oligonucleotide (**ON2**, **ON4**, **ON6** and **ON8**) with a mixture 2.0 μM of each of formylmethyl derivatives of canonical nucleobases (**fmA**, **fmC**, **fmG** and **fmT**) and 2-methylbenzimidazole (**fmB**) at pH of 5.5, ionic strength of 0.10 M and temperature of 23 °C (Scheme 11). Similar reactions were performed on triple-helical models with MOANA or MOGNA residues positioned in the Hoogsteen strand, allowing for a comparative investigation of base filling within the major groove. For single-stranded references, 11-mer oligonucleotides **ON1**, **ON3**, **ON5** and **ON7**, which include only the 3'-end of the hairpins, or the Hoogsteen strands **ON9** and **ON10**, were studied under the same conditions but at a 10-fold higher aldehydic concentration (20 μM). Figure 13 presents the data obtained for the hairpin oligonucleotide **ON2t** as a representative example, with all corresponding UV and extracted ion chromatograms and mass spectrum of the main product.

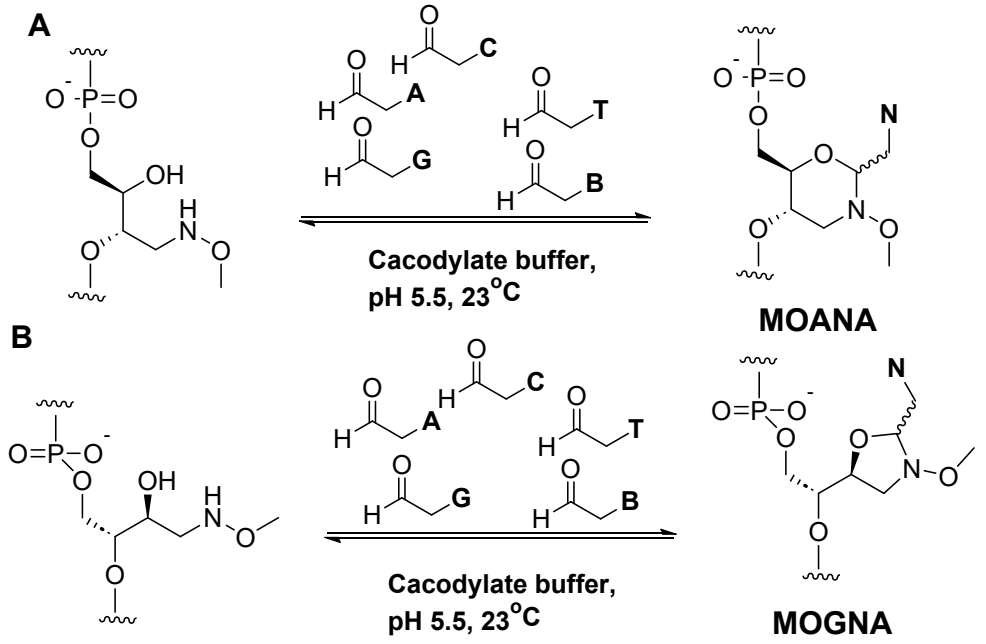

Scheme 11. A dynamic combinatorial assay for studying the incorporation of modified nucleobase aldehydes into an abasic backbone through the formation of (A) N-methoxy-1,3-oxazinane (MOANA) and (B) N-methoxy-1,3-oxazolidine glycol (MOGNA) nucleotide analogues. The assay was performed using a modified oligonucleotide (1.0 μM) incubated with a mixture of aldehydes (fmA, fmC, fmG, fmT, and fmB) (2.0 μM) under the following conditions: T = 23 °C, pH = 5.5 (20 mM cacodylate buffer), and I($NaClO_4$) = 0.10 M for 120 h.

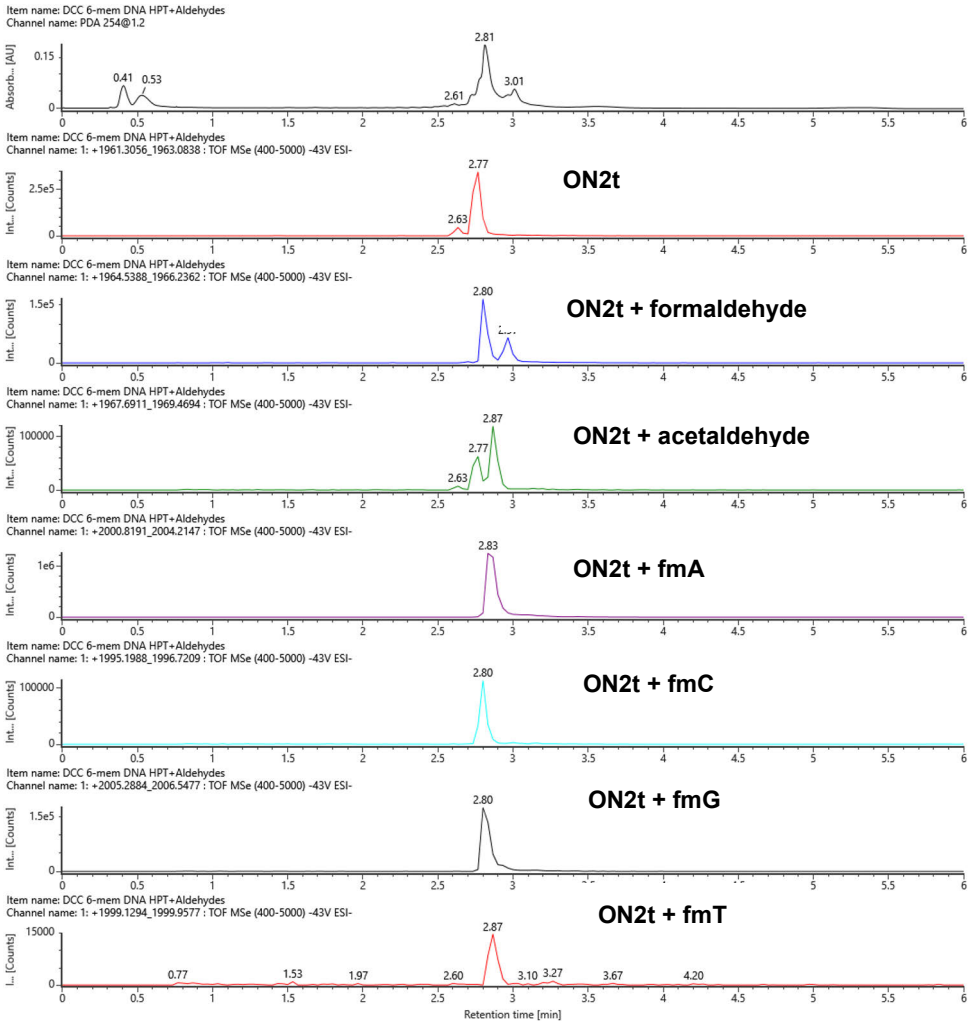

Figure 13. A) Representative UV profile and extracted ion UPLC traces and B) mass spectrum of the main component on incubation of the hairpin oligonucleotide **ON2t** (1.0 μM) with a mixture of aldehydes **fmA, fmC, fmG, fmT** and **fmB** (2.0 μM) at T = 23 °C, pH = 5.5 (20 mM cacodylate buffer) and I(NaClO4) = 0.10 M for 72 h; ACQUITY Premier OST column (50 x 2.1 mm, 1.7 μm); flow rate = 0.4 $mLmin^{-1}$; linear gradient (5—25 % over 4 min) of MeOH in an aqueous solution of hexafluoroisopropanol(40 mM) and triethylamine (7 mM). λ = 254 nm; T = 60 °C.

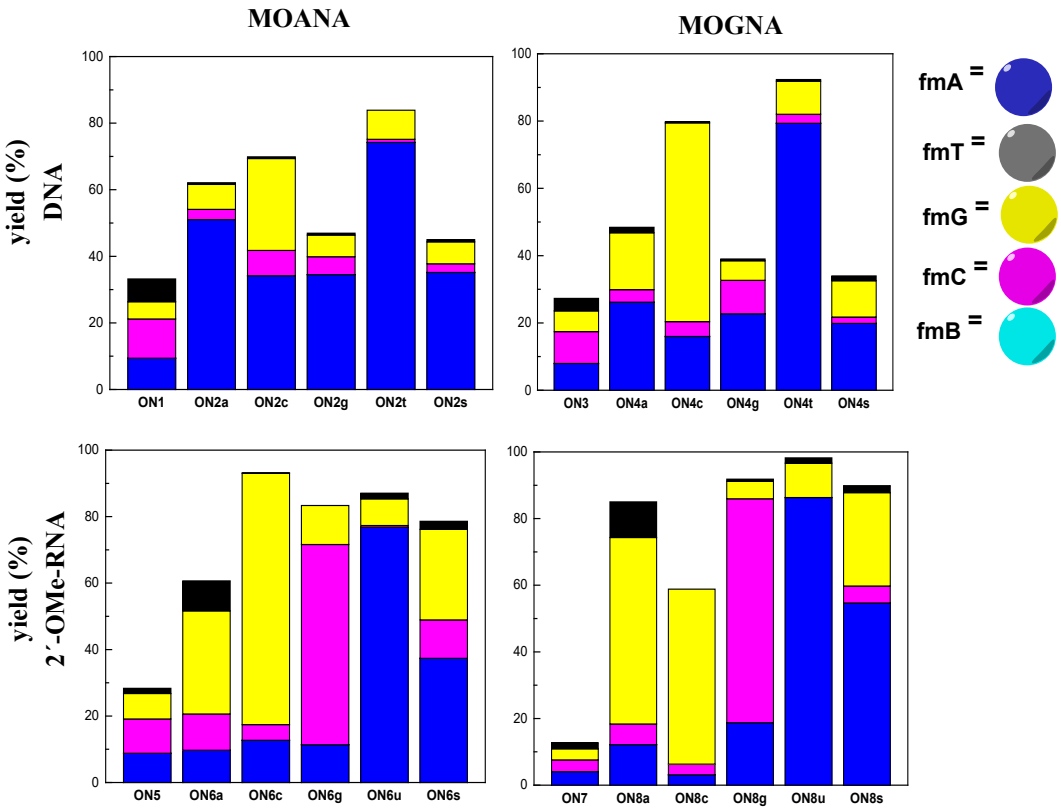

Figure 14. Yields of base-filling A) MOANA—DNA, B) MOGNA—DNA, C) MOANA-2´-OMe- RNA and D) MOANA-2´-OMe-RNA oligonucleotides with a mixture of formylmethylated derivatives of adenine (fmA, blue), cytosine (fmC, magenta), guanine (fmG, yellow) and thymine (fmT, black); [oligonucleotides] = 1.0 μM; [aldehydes] = 20 μM (with the single-stranded oligonucleotides ON1, ON3, ON5 and ON7) / 2.0 μM (with the other oligonucleotides); T = 23 °C; pH = 5.50 (20 mM cacodylate buffer); I(NaClO4) = 0.10 M; reaction time = 120 h. In addition to the derivatives of the canonical nucleobases, 2-(2-methylbenzimidazol-1-yl)acetaldehyde (fmB) was also included in the reaction mixtures but the corresponding base-filling products could not be detected.

Figure 14 provides a summary of the results of base-filling for single-stranded oligonucleotides and duplexes. As anticipated, conversion of the single-stranded control oligonucleotides to aldehyde adducts was low (10–40%) despite the relatively high aldehyde concentration (20 μM). The thymine derivative **fmT** was generally incorporated less efficiently than the other nucleobase derivatives, and the 2-methylbenzimidazole derivative **fmB** was not incorporated at all. No base selectivity was observed in the absence of a template, irrespective of the sequence or backbone chemistry of the single-stranded oligonucleotide.

For MOANA-DNA, the adenine derivative (**fmA**) appears to dominate across all hairpins. The highest base pairing selectivity (88%) with a yield of 74% was

observed with the incorporation of the adenine derivative **fmA** into a hairpin opposite to a thymine residue, aligning with the Watson-Crick base pairing model. The other hairpins, including **ON2a**, **ON2c** and **ON2g**, show a preference for incorporating mismatched **fmA**. **ON2s**, with an abasic site positioned opposite the modified residue, was primarily converted to the **fmA** adduct, achieving a 35% yield with 78% selectivity. Purine-purine mismatches, such as **ON2a-fmA** (55%) and **ON2g-fmA** (37%), demonstrated higher yield compared to pyrimidine-pyrimidine mismatches, such as **ON2c-fmC** (10%) and **ON2t-fmT** (0%). This trend may be attributed to the stabilizing effects of base stacking interactions. Notably, the thymine aldehyde derivative showed little or no incorporation into any of the hairpins, consistent with findings reported in other studies.[235]

The base-filling selectivity of MOGNA-DNA hairpins was similar to that of MOANA-DNA hairpins, with the exception that guanine aldehyde derivative **fmG** incorporated into **ON4c** following Watson-Crick base pairing, yielding 59% with a selectivity of 74%. With **ON4t**, **fmA** incorporated better with 79% yield and 86% selectivity. However, base-filling against purines in MOGNA-DNA hairpins was slightly less efficient compared to their MOANA-DNA counterparts, with overall conversion rates ranging from 40–50%, without a single dominant product in either case. The abasic oligonucleotide hairpin **ON4s** exhibited a reactivity pattern similar to its MOANA counterpart **ON2s**, producing low yields of **fmA** (19%) and **fmG** (10%) adducts, while **fmC** and **fmT** adducts were formed at 1.9% and 1.4% yields, respectively.

In the case of MOANA-2'-OMe-RNA hairpins, base pairing selectivity was improved with either of the purine bases opposite to the modified residue of the oligonucleotide hairpins. For **ON6a**, although the main product was still mismatched (**fmG** at 31% yield), a significant fraction (9%) of the expected **fmT** adduct was also observed, which contrasts with the results on the DNA hairpins. With **ON6g**, incorporation of the Watson-Crick partner **fmC** was favored, though the yield (60%) and selectivity (72%) were still less than ideal. Base filling opposite pyrimidine residues yielded the highest efficiencies, with 75% yield and 81% selectivity for the incorporation of **fmG** into **ON6c**, and 78% yield and 88% selectivity for the incorporation of **fmA** into **ON6u**. Interestingly, the abasic hairpin **ON6s** demonstrated significantly higher reactivity compared to its DNA counterparts, with the **fmA** (37%) and **fmG** (27%) adducts being the predominant products in the mixture.

Changing the base-filling scaffold from MOANA to MOGNA, while retaining the 2'-OMe-RNA backbone, had the most significant effect on the hairpin structure when guanine was positioned opposite the modified residue (**ON8g**). The aldehyde derivative **fmC** demonstrated enhanced incorporation into the hairpin **ON8g**, with selectivity and yield comparable to the aforementioned matched purine nucleobase

derivatives (73% and 67%, respectively). Incorporation of **fmG** into **ON8c** exhibited excellent selectivity (89%), although the yield was relatively modest (52%). For **ON8a, ON8u** and **ON8s**, the product mixtures were essentially the same as those obtained with their MOANA counterparts, but with slightly higher overall conversions.

Our findings show a clear preference for base-filling in double helices with purine derivatives, consistent with prior studies across various backbones and coupling chemistries.[225,235] This is likely driven by base stacking interactions, which are stronger for purines. However, base pairing also plays a significant role, as shown by the selectivity of adenine, cytosine, and guanine derivatives for hairpins that align their canonical Watson–Crick partners opposite to the MOANA or MOGNA residue. This is further supported by the strong discrimination against 2-(2-methylbenzimidazol-1-yl)acetaldehyde (**fmB**), which has a purine-sized stacking surface but lacks the hydrogen bond donors and acceptors necessary for Watson–Crick base pairing. Thymine derivatives consistently exhibited the lowest yield and selectivity. Notably, base-filling discrimination against **fmT** was more pronounced in double helices than in single-stranded oligonucleotides. This may be attributed to the methyl group at the C5 position of thymine, which introduces steric hindrance. In base-filling experiments involving MOANA or MOGNA scaffolds, this methyl group can cause steric clashes with neighboring nucleotides or the backbone, particularly in the compact double-helical environment, making thymine less favorable for incorporation.

The selectivity and yield of base-filling in 2′-O-methyl-RNA hairpins were notably higher compared to their DNA counterparts, particularly with the cytosine derivative **fmC**. This difference can be attributed to the more rigid and pre-organized A-type double-helical structure of 2′-O-methyl-RNA, which reduces the entropic penalty of base-filling. It is also worth noting that peptide nucleic acid (PNA), which is highly suited for base-filling, is similarly pre-organized, facilitating hybridization with both RNA and DNA. PNA-RNA duplexes adopt an A-type structure, while PNA-DNA duplexes exhibit characteristics of both A- and B-type helices, with base pairs displaced from the helical axis—a hallmark of A-type conformations. The influence of the base-filling scaffold—whether MOANA or MOGNA—is more nuanced than the effects of helix geometry and rigidity. In DNA hairpins, the MOGNA scaffold appears to confer certain advantages. However, in the case of 2′-O-methyl-RNA hairpins, the effects are less clear, though the MOGNA scaffold does yield better results with the cytosine derivative **fmC**. The 5-membered oxazolidine ring of the MOGNA scaffold is more flexible than the 6-membered oxazinane ring of the MOANA scaffold. However, this comparison is complicated by the fact that both scaffolds likely exist in a dynamic equilibrium between α and β pseudoanomers. Despite these complexities, the

observed selectivity for base-filling in 2′-O-methyl-RNA hairpins indicates that both scaffolds can effectively position the nucleobase moiety in a manner conducive to Watson–Crick base pairing.

In contrast to the hairpin oligonucleotides, base-filling of the Hoogsteen strand in the triplex assemblies showed little sensitivity to the base pair within the Watson-Crick duplex, regardless of whether the MOANA or MOGNA scaffold was used. Overall conversions were generally below 50%, with no clear selectivity for any specific aldehyde. However, there were some exceptions with the **ON11a•ON12t*ON9** and **ON11a•ON12t*ON10** triplexes, which showed a moderate preference for base-filling with **fmC** (26% and 22%) and **fmG** (29% and 23%). The choice of base-filling scaffold (MOANA or MOGNA) had a minor impact, though slightly higher conversions were observed with MOANA (Figure 15).

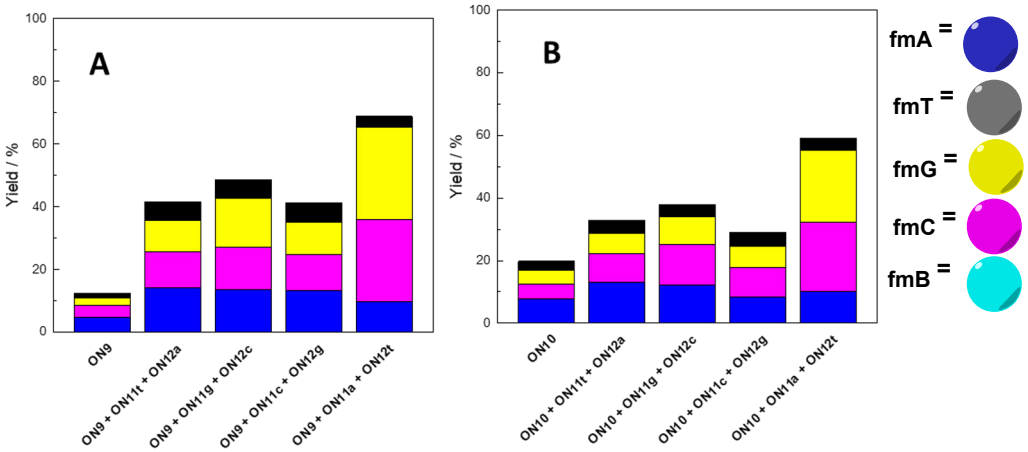

Figure 15. Yields of base-filling A) MOANA—DNA and B) MOGNA—DNA oligonucleotides with a mixture of formylmethylated derivatives of adenine (**fmA**, blue), cytosine (**fmC**, magenta), guanine (**fmG**, yellow) and thymine (**fmT**, black); [oligonucleotides] = 1.0 μM; [aldehydes] = 20 μM (with the single-stranded oligonucleotides **ON9** and **ON10** alone) / 2.0 μM (with the triplex assemblies); T = 23 °C; pH = 5.50 (20 mM cacodylate buffer); *I*($NaClO_4$) = 0.10 M; reaction time = 120 h. In addition to the derivatives of the canonical nucleobases, 2-(2-methylbenzimidazol-1-yl)acetaldehyde (**fmB**) was also included in the reaction mixtures but the corresponding base-filling products could not be detected.

3.9 Duplex stability of oligonucleotide hairpin-**fA** and -**fmA** conjugates

The base-filling experiments demonstrated a strong preference for the incorporation of **fA** or **fmA** into the hairpin oligonucleotides with either thymine or uracil residue opposite to the MOANA or MOGNA site. The melting temperatures of all hairpin **ON2-fA** conjugates (**ON2a + fA, ON2c + fA, ON2g + fA, ON2t + fA and ON2s + fA)** were measured to investigate the effect of a single MOANA residue on the stability of the DNA double helix. The samples were prepared at 500 μM concentration of both the oligonucleotide and the aldehyde and preincubated for 120 hours at 23 °C. After incubation, the reaction mixtures were diluted to 1.0 μM concentration by addition of 20 mM cacodylate buffer (pH = 7.4), the ionic strength of which had been adjusted to 0.10 M with $NaClO_4$. For reference, a set of samples of the naked hairpins **ON2** without **fA** was also prepared. Similar studies were conducted on **MOANA-DNA** and **MOGNA-DNA** hairpin oligonucleotides (**ON2a, ON2c, ON2g ON2s and ON2t** and **ON4a ON4c ON4g ON4s,** and **ON4t**) with **fmA**. Each hairpin (1.0 μM) was incubated with two equivalents of the adenine derivative **fmA** at 23 °C and pH 5.5 for 120 hours after which the pH of the solutions was adjusted to 7.4. Melting profiles were acquired by recording the absorbance at 260 nm over a temperature range of 10–90 °C.

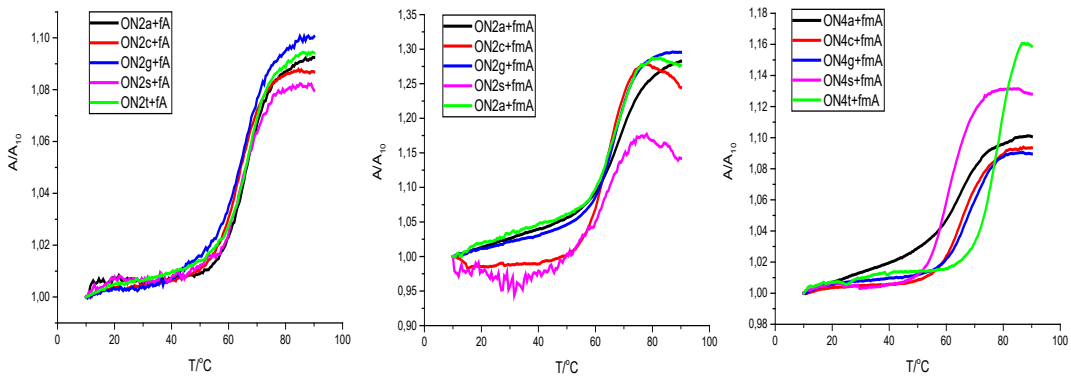

Figure 16. Melting temperatures of the hairpin oligonucleotides A) **ON2a**, **ON2c**, **ON2g**, **ON2s** and **ON2t** in the presence of the aldehyde **fA**; B) **ON2a**, **ON2c**, **ON2g**, **ON2s** and **ON2t** and C) **ON4a**, **ON4c**, **ON4g**, **ON4s** and **ON4t** and their base-filling products with aldehyde **fmA**; [oligonucleotides] = 1.0 μM; pH = 7.4 (20 mM cacodylate buffer); *I*($NaClO_4$) = 0.10 M.

Table 5. Melting temperatures of the hairpin oligonucleotides **ON2a**, **ON2c**, **ON2g**, **ON2t** and **ON2s**, **ON4a**, **ON4c**, **ON4g**, **ON4s** and **ON4t**, **ON6a**, **ON6c**, **ON6g**, **ON6s** and **ON6u**, **ON8a**, **ON8c**, **ON8g**, **ON8s** and **ON8u**) in the absence and presence of the aldehyde **fA** or **fmA**; [oligonucleotides] = 1.0 μM; [**fA**] = 0/1.0 μM; pH = 7.40 (20 mM cacodylate buffer); *I*($NaClO_4$) = 0.10 M.

Oligos	T_m (**naked**)/°C	T_m (**+fA**)/°C	T_m (**+fmA**)/°C	ΔT_m (**+fA**)/°C	ΔT_m(**+fmA**)/°C
ON2a	66.6 ± 0.1[a]	66.2 ± 0.1	67.9 ± 0.3	-0.4	1.3
ON2c	63.9 ± 0.1[a]	63.9 ± 0.1	64.4 ± 0.3	0	0.5
ON2g	67.4 ± 0.1[a]	65.0 ± 0.1	66.7 ± 0.3	-2.4	-0.7
ON2t	64.2 ± 0.1[a]	66.7 ± 0.1	66.5 ± 0.3	2.5	2.3
ON2s	64.7 ± 0.1[a]	64.4 ± 0.4	62.8 ± 0.3	-0.3	-1.9
ON4a	66.7 ± 0.1	n.a[b]	60.7 ± 0.1	n.a[b]	-6
ON4c	65.9 ± 0.4	n.a[b]	61.0 ± 0.2	n.a[b]	-4.9
ON4g	68.8 ± 0.2	n.a[b]	62.9 ± 0.1	n.a[b]	-5.9
ON4t	64.7 ± 0.1	n.a[b]	64.2 ± 0.1	n.a[b]	-0.5
ON4s	66.9 ± 0.1	n.a[b]	61.7 ± 0.1	n.a[b]	-5.2
ON6a	83.2 ± 0.1	n.a[b]	n.a[b]	n.a[b]	n.a[b]
ON6c	77.8 ± 0.1	n.a[b]	n.a[b]	n.a[b]	n.a[b]
ON6g	83.0 ± 0.1	n.a[b]	n.a[b]	n.a[b]	n.a[b]
ON6u	79.3 ± 0.1	n.a[b]	n.a[b]	n.a[b]	n.a[b]
ON6s	79.5 ± 0.1	n.a[b]	n.a[b]	n.a[b]	n.a[b]
ON8a	83.4 ± 0.1	n.a[b]	n.a[b]	n.a[b]	n.a[b]
ON8c	80.7 ± 0.1	n.a[b]	n.a[b]	n.a[b]	n.a[b]
ON8g	83.7 ± 0.2	n.a[b]	n.a[b]	n.a[b]	n.a[b]
ON8u	80.2 ± 0.5	n.a[b]	n.a[b]	n.a[b]	n.a[b]
ON8s	79.8 ± 0.1	n.a[b]	n.a[b]	n.a[b]	n.a[b]

[a] The average results of the **ON2** series were obtained from experiments conducted in different buffer solutions under otherwise the same conditions.
[b] Not determined.

Table 5 summarizes the melting temperatures (**T_m**) of modified oligonucleotides incorporating 9-**formyl**-9-**deazaadenine (fA)** or **adenine** acetaldehyde **(fmA)**, along with the differences in melting temperature (**ΔT_m**) compared to the unmodified (**naked**) sequences. All hairpin-**fA** and **fmA** conjugates showed monophasic sigmoidal melting profiles (Figure 16). Incorporation of **fA** into **ON2a** and **ON2s** led to a slight decrease in melting temperature (ΔT_m = -0.4 and -0.3 °C, respectively), indicating a minor destabilization of the duplex. **ON2t-fA** showed the greatest stabilization (ΔT_m = +2.5 °C), while **ON2g-fA** exhibited the most significant destabilization (ΔT_m = -2.4 °C). With the **ON2c** hairpin, the **fA** conjugate showed no change in stability (ΔT_m = 0.0 °C). In evaluating the impact of **fmA** on the **ON2**

series, the greatest stabilization was observed in **ON2t-fmA (ΔT_m = +2.3 °C)**, again consistent with Watson-Crick base pairing. **ON2a-fmA** also exhibited significant stabilization with a **ΔT_m of +1.3 °C**. Conversely, the highest destabilization occurred when **fmA** was incorporated into **ON2s (ΔT_m = -1.9 °C)**. Incorporation of **fmA** into **ON2c and ON2g** resulted in **modest stabilization (+0.5°C) and destabilization (-0.7°C),** respectively. For the **ON4** series, significant decreases in T_m were observed with **fmA** incorporation into **ON4a** (ΔT_m = -6.0 °C), **ON4c** (ΔT_m = -4.9 °C), **ON4g** (ΔT_m = -5.9 °C) and **ON4s** (ΔT_m = -5.2 °C). The most substantial destabilization was seen in **ON4a**+**fmA** (ΔT_m = -6.0 °C) and **ON4g**+**fmA** (ΔT_m = -5.9 °C), indicating that these modifications are particularly disruptive to the oligonucleotide structure. The **ON4t-fmA** conjugate also showed slight destabilization (ΔT_m = -0.5 °C), but much less than the mismatched conjugates. In the case of 2′-*O*-methyl-RNA hairpins, the melting temperatures were high, exceeding 80 °C and the curves were not levelling off even at 90 °C. Due to their exceptional stability even in their naked form, the 2-*O*-methyl-RNA hairpins were considered unsuitable for studying the effects of base-filling. As a result, the impacts of base filling experiments were focused exclusively on the DNA hairpins.

4 Conclusion

The reversible base-filling of *N*-methoxy-1,3-oxazinane (MOANA) and *N*-methoxy-1,3-oxazolidine glycol nucleic acids (MOGNA) has proven to be a viable approach for preparing oligonucleotide-conjugates. The required (2R,3S)-4-(methoxyamino)butane-1,2,3-triol-modified oligonucleotides can be conveniently synthesized using an automated synthesizer, achieving yields of 77–99% for coupling of the modified building block. Two isomers of this reactive scaffold were used, resulting in either an *N*-methoxy-1,3-oxazinane (MOANA) or an *N*-methoxy-1,3-oxazolidine glycol (MOGNA) nucleoside analogue via cyclization with aldehyde-derivatized nucleobases. The formation of MOANA and MOGNA conjugates is dynamically reversible under slightly acidic pH (5.5) but the products are relatively stable at neutral pH (7.4). Moreover, the reaction rate and equilibrium vary with the properties of the aldehydes.

Base filling of single-stranded oligonucleotides showed low efficiency, with conversions ranging from 10 to 40%, even at relatively high aldehyde concentrations. Moreover, no selectivity for any particular nucleobase aldehyde was observed without a templating strand. Overall, the yield and selectivity of base-filling were consistently higher with the relatively rigid 2′-OMe-RNA than with the more flexible DNA backbone, regardless of whether the MOGNA or MOANA scaffold was used. Adenine acetaldehyde consistently incorporated with high yield and selectivity, especially when paired with thymine or uracil, in line with the Watson-Crick base pairing model. Cytosine acetaldehyde showed significantly better incorporation into 2′-OMe-RNA-MOGNA and 2′-OMe-RNA-MOANA than into a DNA-MOANA duplex. Guanine acetaldehyde was efficiently incorporated into most hairpins, except in DNA-MOANA, where yields were notably lower. The Watson–Crick base-pairing along with a high stacking contribution of purine nucleobases appears to be important for the yield and selectivity. Thymine acetaldehyde was poorly incorporated overall, though slightly better in 2′-OMe-RNA than in DNA, consistent with previous report.[235] Mismatches such as A-A and G-G were prevalent, highlighting a preference for purine-purine over pyrimidine-pyrimidine base pairing. 2-Methlybenzimidazole acetaldehyde, an analogue of adenine acetaldehyde with no hydrogen bond donors or acceptors, did not show any

incorporation. Conversely, the effects of the two isomers of the (2R,3S)-4-(methoxyamino)butane-1,2,3-triol scaffold (MOANA vs. MOGNA) on base-pairing selectivity were modest and varied depending on the sequence.

The incorporation of 9-formyl-9-deazeadenine and adenine acetaldehyde opposite to a thymine within a MOANA-DNA hairpin resulted in increased melting temperatures of +2.5 °C and +2.3 °C, in line with canonical Watson-Crick base pairing. In the MOGNA-DNA hairpins, a general trend of decreased stability was observed upon incorporation of adenine acetaldehyde. However, a smaller destabilization was observed for base-filling opposite to thymine, again consistent with Watson-Crick base pairing.

The method developed in this work can be applied to produce and screen a broad range of oligonucleotides with diverse modifications. More broadly, the use of oxazinane/oxazolidine-based DCC is a promising technique with numerous potential applications in the discovery of DNA-binding molecules. The pH-dependent reactivity of *N*-methoxy-1,3-oxazinanes and -oxazolidines makes it a valuable tool for generating dynamic combinatorial libraries. Potential applications include identification of single-nucleotide polymorphisms (SNPs), antisense therapies, CRISPR-Cas gene-editing systems, peptide-oligonucleotide chimeras or modified aptamers and DNAzymes.

5 Materials and Methods

5.1 General Methods

Air and moisture-sensitive reactions were performed using oven-dried glassware under inert nitrogen atmosphere. All the reagents for the syntheses were commercial products and were used as received. Solvents used in organic synthesis were of reagent grade and dried over 3 or 4 Å molecular sieves. The reactions were monitored by thin layer chromatography (TLC) performed on Merck 60 (silica gel F254) plates. TLC plates were visualized by exposure to ultraviolet light. Purification of products was accomplished using column chromatography on silica gel (230-400 mesh). Freshly distilled triethylamine was for used for HPLC elution buffers. Mass spectra were recorded on a micrOTOF-Q ESI-MS and Waters Acquity RDa mass spectrometer. ^{1}H, ^{13}C and ^{31}P NMR spectra were recorded on Bruker Avance 500 and 600 NMR spectrometers and chemical shifts are given in ppm. Detailed characterization of synthesized compounds is provided in the original publications.

5.2 Oligonucleotide synthesis

The oligonucleotides were synthesized on an ÄKTA Oligopilot Plus 10 DNA/RNA synthesizer by conventional phosphoramidite strategy. In the case of **ON1**, phosphoramidite building block **14** was used. The coupling proceeded with 64% efficiency. Phosphoramidite **17** was used in the syntheses of **ON2a, ON2c, ON2g ON2s** and **ON2t**. Based on the trityl response, the coupling efficiency was 99%. Phosphoramidites **20** and **23** were used for the syntheses of oligonucleotides **ON3**, **ON4a**, **ON4c**, **ON4g**, **ON4t** and **ON4s** and **ON5**, **ON6a**, **ON6c**, **ON6g**, **ON6u**, **ON6s**, **ON7**, **ON8a**, **ON8c**, **ON8g**, **ON8u** and **ON8s.** The coupling efficiency for the phosphoramidite building blocks **20** and **23** were 77-99%. After chain assembly, the cleavage of oligonucleotides from the solid support and the phosphate and base protections of the modified building block removed by incubation in 25 % aqueous NH_3 at 55 °C between 16 -18 h.

Purification of the modified oligonucleotides **ON1**, **ON2a, ON2c, ON2g, ON2s,** and **ON2t** by RP-HPLC on a HypersilODS C18 column (250 × 10 mm, 5 µm) eluting with a linear gradient (5—20 % over 25 min, flow rate = 3.0 mL min^{-1}) of acetonitrile

in 50 mM aqueous triethylammonium acetate (pH = 7.0), the detection wavelength being 260 nm. For modified oligonucleotide **ON1**, the base, phosphate group and the Fmoc protection of the methoxyamino group were quantitively removed but the TBDMS protection was not which enable in the separation of the full-length from the truncated sequences of the oligonucleotides. The purified oligonucleotide was desilylated by conventional treatment with triethylamine trihydrofluoride in dimethylsulfoxide, and passed through an RP-HPLC column again using the aforementioned conditions to yield the pure product.

Purification of modified oligonucleotides **ON3**, **ON4a**, **ON4c**, **ON4g**, **ON4t** and **ON4s** and **ON5**, **ON6a**, **ON6c**, **ON6g**, **ON6u**, **ON6s**, **ON7**, **ON8a**, **ON8c**, **ON8g**, **ON8u** and **ON8s** were carried out by using reverse phase HPLC on a Hypersil ODS C18 column (250 × 4.6 mm, 5 μm) upon elution with a linear gradient of acetonitrile (10–40 % over 25 min, flow rate 3.0 mL min^{-1}) in 50 mmol L^{-1} aqueous triethylammonium acetate. The paranitrobenzylidene group was removed by acidification using acetic acid and incubating for 5 days. The oligonucleotides were passed through an RP-HPLC column again using the aforementioned conditions to yield the pure products.

The identities of the purified oligonucleotides **ON1, ON2a, ON2c, ON2g, ON2s,** and **ON2t** were confirmed using ESI-TOF-MS. In the case of modified oligonucleotides **ON3, ON4a, ON4c, ON4g, ON4t,** and **ON4s,** as well as **ON5, ON6a, ON6c, ON6g, ON6u, ON6s, ON7, ON8a, ON8c, ON8g, ON8u,** and **ON8s** the identities were characterized by UPLC-ESI-TOF-MS. All the synthesized oligonucleotides were quantified using UV spectrophotometry.

5.3 UV Melting temperature studies

The UV melting curves was obtained by measuring the absorbance as a function of temperature at 260 nm on a PerkinElmer Lambda 35 UV-vis spectrophotometer equipped with a Peltier temperature controller using quartz cuvettes with 10 mm optical path length. The temperature was changed at a rate of 0.5 °C min^{-1} from 10 to 90 °C. The measurements were carried out at pH 5.5 and 7.4 in 20 mM cacodylate buffer with ionic strength of 0.1 M, adjusted with $NaClO_4$. Thermal stabilities were evaluated for the hairpin oligonucleotides **ON2a**, **ON2c**, **ON2g**, **ON2t** and **ON2s** (1.0 μM) in the absence and presence of the aldehyde **fA** (0 / 1.0 μM). Subsequently, the thermal stabilities of **ON2a**, **ON2c**, **ON2g**, **ON2t**, **ON2s**, **ON4a**, **ON4c**, **ON4g**, **ON4t** and **ON4s** (1.0 μM) were assessed in the absence and presence of the aldehyde **fmA** (0 / 1.0 μM). Melting temperatures for the 2'-OMe-RNA–MOANA and 2'-OMe-RNA–MOGNA hairpins **ON6a, ON6c, ON6g, ON6u and ON6s** and **ON8a, ON8c, ON8g, ON8u and ON8s** and the triplexes **ON11t · ON12a*ON9**, **ON11g · ON12c*ON9**, **ON11c · ON12g*ON9** and **ON11a · ON12t*ON9** and

ON11t · ON12a*ON10, **ON11g · ON12c*ON10**, **ON11c · ON12g*ON10** and **ON11a · ON12t*ON10** were determined only in the absence of any aldehydes. The Watson-Crick and Hoogsteen T_m values were determined as inflection points on the UV melting curves.

5.4 Kinetic and equilibrium studies

Both kinetic and equilibrium studies on aldehydes **fA**, **fU** and **fI** were performed by first preparing a 500 μM stock solution of the aldehyde and a hairpin oligonucleotide (**ON2a**, **ON2c**, **ON2g**, **ON2t** or **ON2s**). The reaction mixtures were prepared by mixing appropriate volumes of stock solutions of the oligonucleotide in H_2O and the aldehyde in either DMSO (for **fA** and **fI**) or H_2O (for **fU**). The mixtures were lyophilized to dryness. The residues were dissolved in a 200 mM aqueous triethylammonium acetate buffer (pH = 5.5) and the resulting solutions incubated at 23 °C for either 48 (in the case of **fA**) or 120 h (in the case of **fU** and **fI**). The dissociation rates of hairpin-aldehyde conjugates were analyzed by diluting the 500 μM stock solutions to 1.0 μM with 200 mM aqueous triethylammonium acetate buffer (pH = 5.5). The resulting solutions were analyzed at diffrerent time intervals using RP-HPLC on a Thermo Scientific Hypersil ODS C18 column (250 × 4.6 mm, 5 μm). Separation was achieved with a linear gradient of MeCN in 50 mM aqueous triethylammonium acetate buffer (pH = 7.0) at a flow rate of 1.0 mL min^{-1}. For **fA** and **fU**, the MeCN content was increased from 5% to 29% over 15 minutes. For the more hydrophobic **fI**, this gradient was followed by a steeper increase from 29% to 40% over 5 minutes, and finally 5 minutes of isocratic elution at 40%. Detection wavelengths were set at 260 nm for **fA** and **fU** and 300 nm for **fI**. The retention times were 6.9 min (**fA**), 4.2 min (**fU**), 18.5 min (**fI**), and 8.5 min (oligonucleotides). Peak areas of the aldehydes were normalized against the total peak area and plotted as a function of time. Dissociation rate constants were determined by non-linear least squares fitting of these data to a first-order rate law. The kinetics and equilibria of conversion of each oligonucleotide (**ON2t**, **ON4t**, **ON6u** and **ON8u**) to its adenine acetaldehyde (**fmA**) adduct were determined at pH 5.5 in 20 mM cacodylate buffer, with an ionic strength of 0.10 M ($NaClO_4$). The reaction mixtures contained a 1.0 μM concentration of the oligonucleotides and a 2.0 μM concentration of **fmA**. The resulting solutions were analyzed at different time intervals using RP-HPLC on an ACQUITY Premier OST column (50 × 2.1 mm, 1.7 μm). The analysis was performed at a flow rate of 0.4 mL/min under a linear gradient of 5–25% MeOH over 4 minutes in an aqueous solution of hexafluoroisopropanol (40 mM) and triethylamine (7 mM). Detection was carried out at λ = 254 nm with a column temperature of 60°C. In each case, the starting material exhibited first-order disappearance, resulting in the formation of N-methoxy-1,3-oxazinanes and N-

methoxy-1,3-oxazolidines. The observed half-lives ranged from 9 to 32 hours, showing no clear correlation with the backbone structure. A reaction time of 120 hours, corresponding to approximately 4–13 half-lives, was considered sufficient for the DCC reactions. In each case, the formation of the expected conjugates was confirmed using UPLC-MS.

5.5 Dynamic combinatorial chemistry

The DCC reaction mixtures were prepared by diluting the appropriate oligonucleotide to a 1.0 μM concentration in a mixture of aldehydes (**fmA, fmC, fmG, fmT and fmB**) at different concentrations depending on the oligonucleotide type: 20 μM for single-stranded oligonucleotides (**ON1, ON3, ON5 and ON7**) and 2.0 μM for both duplex (**ON2, ON4, ON6 and ON8**) and triplex (**ON9 and ON10**) oligonucleotides. The reaction was carried out in 20 mM cacodylate buffer (pH = 5.5), with the ionic strength adjusted to 0.10 M using $NaClO_4$. The reaction mixtures were incubated at 23 °C for at least 120 h, after which their compositions were analyzed by UPLC-ESI-MS. The composition of the DCL, consisting of the naked oligonucleotides and their various base-filling products, was determined by integrating the extracted ion ($[M–2H]^{2–}$ for the 11-mers, $[M–3H]^{3–}$ for the Hoogsteen strands and $[M–4H]^{4–}$ for the hairpins) chromatograms. Quantification was performed under the assumption of equal ionizability for closely related structures.

Acknowledgements

This thesis is based on experimental work conducted in the Laboratory of Organic Chemistry and Chemical Biology at the Department of Chemistry, University of Turku, Finland, during the years 2020–2025. I am deeply grateful to the Department of Chemistry at the University of Turku for providing the infrastructure, resources and a conducive environment that fostered scientific exploration and learning. Your unwavering support has been instrumental in enabling me to achieve this academic milestone.

First and foremost, I express my profound gratitude to Almighty God and my Saviour, Jesus Christ. His grace, guidance, and strength have been my anchor throughout this PhD academic journey. Without His divine blessings and grace, this work would not have been possible (1 Corinthians 15:10).

I am deeply indebted to my PhD supervisor, Professor Tuomas Lönnberg, for giving me the opportunity to pursue a doctoral degree under his guidance and leadership. Your immense knowledge, experience and expertise in nucleic acid chemistry have been a tremendous asset to this work. Thank you for your continuous patience, encouragement, thoughtful guidance, support and trust in me throughout these years. You consistently encouraged me to understand the deeper reasons behind every concept and the mechanisms of every reaction, inspiring me to think critically and holistically. Your dedication and generosity in sharing your time, knowledge, and expertise have been truly remarkable. I am equally grateful to my second supervisor and research director, Professor Pasi Virta, for your inspiration, invaluable advice, and unwavering support.

I would like to extend my sincere thanks to Professor Kari Rissanen and Associate Professor Hiromu Kashida for their meticulous review and evaluation of my thesis. Your insightful comments and suggestions were instrumental in refining this work. I am also grateful to Professor Juan José Díaz Mochón for graciously accepting the role of opponent in my public PhD defense.

My heartfelt gratitude goes to the entire Bioorganic Chemistry Group, both past and present members, for your collaboration, camaraderie, and support throughout my doctoral research. I am especially thankful to Dr. Lange Saleh, Dr. Aapo Aho, Dr. Asmo Aro-Heinilä, Dr. Antti Äärelä, Dr. Dattatraya Ukale, Hanni Haapsaari,

Heidi Kähkölä, Dr. Tharun Kotammagari, Tommi Österlund, Toni Laine, Verneri Saari, Razieh Moosavi, Müjgan Üstbas, Dr. Vijay Gulumkar, Dr. Ville Tähtinen, Dr. Madhuri Hande, Dr. Mikko Ora, Dr. Satu Mikkola and Dr. Petja Rosenqvist. Your contributions, support, and friendship made this journey both productive and memorable.

I owe special thanks to my beloved wife, Deborah Afari. As the saying goes, "Behind every successful man is a strong woman." You have been my rock throughout this journey, providing unwavering financial and emotional support. Your prayers, encouragement, patience, sacrifices, and unconditional love are beyond measure. Thank you for standing by me through every challenge and celebrating every success with me. I am truly blessed by your generosity and dedication. May the Lord bless you abundantly for your immense contributions to my life and this achievement.

I extend my warm gratitude to the members of the Material and Intelligent Material Chemistry groups, whose collaboration and insightful discussions have been invaluable. I am particularly grateful to Cecilia Degbe, Dr. Adefunke Koyejo, Sachin Kochrekar, Dr. Rahul Yewale, Dr. Plawan Jha, Dr. Sami Vuori, Majid Al-waeel, Narhari Sapkota, and Vinh Nguyen. Your camaraderie and contributions fostered a positive work environment and enriched this experience.

I also wish to thank Kirsi Laaksonen and Tiina Buss for ensuring the seamless supply of chemicals and equipment during my experiments. My gratitude extends to Dr. Alex Dickens, Dr. Jani Rahkila, Dr. Denys Mavrynsky, and Tuomas Karskela at the Instrument Center/CCMA for their assistance with MS and NMR measurements.

Special thanks to my church family at the Deeper Life Bible Church in Finland, particularly Pastor Dr. James Anyan, the national overseer, and Pastor Dr. Sunday Olaleye, Pastor Joe Dabol, Pastor Biliaminu Jimoh, Pastor Dr. Dandison Ukpabi, Pastor Dr. Promise Mpamah, Pastor Dr. Bright Ankudze, Pastor Dr. Cheneso Moumakwa, Pastor Dr. Richard Agyei, Pastor Dr. Albert Ofori, Pastor Emmanuel Agamah, Pastor Brian Bowa Zyambo, Pastor Akwesi Adusei, Pastor Theophilus Alale, Pastor Innocent, Pastor Kayode Asoro, Pastor Francis Boafo, Mrs. Aba Anyan, Mrs. Esther Olaleye, Mrs. Mary Jimoh, Mrs. Grace Dandison Ukpabi, Mrs. Yaa Asantewaa Ofori, Mrs. Juliet Mpamah, Mrs. Cecilia Agamah, Mrs. Esther Adusei, Mrs. Yemisi Asoro, Mrs. Christine Kanyika Zyambo, Mrs. Benedicta Alale Mrs. Esther Agyei and all members of the congregation. Your prayers, encouragement, and wise counsel have been a guiding light throughout my journey. I also appreciate the youth leaders, including Sis. Mercy Ankudze, Sis. Deborah Afari, Sis. Purity Boafo, and Sis. Victoria, Sis. Esther Barika, Bro. Ernest and Dr. William for their dedication and support for the youth ministry. May the Lord richly bless you for your service and sacrifices.

I am deeply thankful to my mother, Regina Adu Yeboah, and my siblings, Eric Amoah, Mavis Ofosuhemaah, Mina Amponsah, and Comfort Awisi, for your prayers and encouragement. My gratitude also extends to my in-laws, Mr. Jacob Offei Kwafo, Mrs. Elizabeth Kwafo, Benedicta Kwafo, Esther Kwafo and Rosina Kwafo for their love and support.

Finally, I would like to extend my heartfelt gratitude to the Ghanaian communities in Turku and beyond, especially the Ghana Union-Turku and all Ghanaians in Finland. Your support, friendship, and encouragement have been an integral part of my life throughout this journey, and I am deeply thankful for the sense of belonging and strength you have provided. To everyone who contributed in ways both big and small, I am forever grateful. This thesis is as much yours as it is mine.

Turku, August 2025
Mark Nana Kwame Afari

List of References

[1] S. Minchin, J. Lodge, *Essays Biochem.* **2019**, *63*, 433–456.
[2] F. Gebauer, M. W. Hentze, *Nat. Rev. Mol. Cell Biol.* **2004**, *5*, 827–835.
[3] J. Gómez-Márquez, *FEBS J.* **2010**, *277*, 3451–3451.
[4] L. Finzi, W. K. Olson, *Biophys. Rev.* **2016**, *8*, 1–3.
[5] E. Jabri, *Nat. Rev. Mol. Cell Biol.* **2005**, *6*, 361–361.
[6] N. Bettin, C. Oss Pegorar, E. Cusanelli, *Cells* **2019**, *8*, 246.
[7] J. H. Bergmann, D. L. Spector, *Curr. Opin. Cell Biol.* **2014**, *26*, 10–18.
[8] M. Kaushik, S. Kaushik, K. Roy, A. Singh, S. Mahendru, M. Kumar, S. Chaudhary, S. Ahmed, S. Kukreti, *Biochem. Biophys. Rep.* **2016**, *5*, 388–395.
[9] M. D. Frank-Kamenetskii, S. M. Mirkin, *Annu. Rev. Biochem.* **1995**, *64*, 65–95.
[10] G. Felsenfeld, D. R. Davies, A. Rich, *J. Am. Chem. Soc.* **1957**, *79*, 2023–2024.
[11] K. Mizuuchi, M. Mizuuchi, M. Gellert, *J. Mol. Biol.* **1982**, *156*, 229–243.
[12] N. Panayotatos, R. D. Wells, *Nature* **1981**, *289*, 466–470.
[13] A. J. Courey, J. C. Wang, *J. Mol. Biol.* **1988**, *202*, 35–43.
[14] J. Spiegel, S. Adhikari, S. Balasubramanian, *Trends Chem.* **2020**, *2*, 123–136.
[15] H. J. Lipps, D. Rhodes, *Trends Cell Biol.* **2009**, *19*, 414–422.
[16] D. Rhodes, H. J. Lipps, *Nucleic Acids Res.* **2015**, *43*, 8627–8637.
[17] A. Rich, A. Nordheim, A. H.-J. Wang, *Annu. Rev. Biochem.* **1984**, *53*, 791–846.
[18] C. K. Singleton, J. Klysik, S. M. Stirdivant, R. D. Wells, *Nature* **1982**, *299*, 312–316.
[19] R. E. Dickerson, H. R. Drew, B. N. Conner, R. M. Wing, A. V. Fratini, M. L. Kopka, *Science* **1982**, *216*, 475–485.
[20] B. D. Adams, C. Parsons, L. Walker, W. C. Zhang, F. J. Slack, *J. Clin. Invest.* **2017**, *127*, 761–771.
[21] M. Matsui, D. R. Corey, *Nat. Rev. Drug Discov.* **2017**, *16*, 167–179.
[22] J. Sana, P. Faltejskova, M. Svoboda, O. Slaby, *J. Transl. Med.* **2012**, *10*, 103.
[23] D. Moazed, *Nature* **2009**, *457*, 413–420.
[24] S. Valadkhan, *Curr. Opin. Chem. Biol.* **2005**, *9*, 603–608.
[25] K. M. Vasquez, G. Wang, *Mutat. Res./Fundam. Mol. Mech. Mutagen.* **2013**, *743–744*, 118–131.
[26] J. Zhao, A. Bacolla, G. Wang, K. M. Vasquez, *Cell. Mol. Life Sci.* **2010**, *67*, 43–62.
[27] G. Wang, K. M. Vasquez, *Mutat. Res./Fundam. Mol. Mech. Mutagen.* **2006**, *598*, 103–119.
[28] G. Wang, K. M. Vasquez, *DNA Repair* **2014**, *19*, 143–151.
[29] A. G. Matera, R. M. Terns, M. P. Terns, *Nat. Rev. Mol. Cell Biol.* **2007**, *8*, 209–220.
[30] S. Valadkhan, L. S. Gunawardane, *Essays Biochem.* **2013**, *54*, 79–90.
[31] G. T. Williams, F. Farzaneh, *Nat. Rev. Cancer* **2012**, *12*, 84–88.
[32] J. Liang, J. Wen, Z. Huang, X. Chen, B. Zhang, L. Chu, *Front Oncol.* **2019**, *9*, 1–9.
[33] J. van der Werf, C. Chin, N. Fleming, *Biology* **2021**, *10*, 809.
[34] M. Wajahat, C. P. Bracken, A. Orang, *Int. J. Mol. Sci.* **2021**, *22*, 10193.
[35] L. Statello, C.-J. Guo, L.-L. Chen, M. Huarte, *Nat. Rev. Mol. Cell Biol* **2021**, *22*, 159–159.
[36] M. C. Bridges, A. C. Daulagala, A. Kourtidis, *J. Cell Biol.* **2021**, *220*, 1–17.

[37] T. X. Lu, M. E. Rothenberg, *J. Allergy Clin. Immunol.* **2018**, *141*, 1202–1207.
[38] T. Cao, X. Zhen, *CNS Neurosci. Ther.* **2018**, *24*, 586–597.
[39] C. Backes, E. Meese, A. Keller, *Mol. Diagn. Ther.* **2016**, *20*, 509–518.
[40] J. J. Rossi, D. J. Rossi, *Molecular Therapy* **2021**, *29*, 431–432.
[41] S. T. Crooke, J. L. Witztum, C. F. Bennett, B. F. Baker, *Cell Metab.* **2018**, *27*, 714–739.
[42] M. J. Piatek, A. Werner, *Biochem. Soc. Trans.* **2014**, *42*, 1174–1179.
[43] Y. Liu, M. Dou, X. Song, Y. Dong, S. Liu, H. Liu, J. Tao, W. Li, X. Yin, W. Xu, *Mol. Cancer* **2019**, *18*, 123.
[44] Y. W. Iwasaki, M. C. Siomi, H. Siomi, *Annu. Rev. Biochem.* **2015**, *84*, 405–433.
[45] B. Czech, M. Munafò, F. Ciabrelli, E. L. Eastwood, M. H. Fabry, E. Kneuss, G. J. Hannon, *Annu. Rev. Genet.* **2018**, *52*, 131–157.
[46] Y. Xie, W. Dang, S. Zhang, W. Yue, L. Yang, X. Zhai, Q. Yan, J. Lu, *Mol. Cancer* **2019**, *18*, 37.
[47] Y. L. Chu, H. Li, P. L. A. Ng, S. T. Kong, H. Zhang, Y. Lin, W. C. S. Tai, A. C. S. Yu, A. K. Y. Yim, H. F. Tsang, W. C. S. Cho, S. C. C. Wong, *Expert Rev. Mol. Diagn.* **2020**, *20*, 665–678.
[48] W. Chang, J. Wang, *Cells* **2019**, *8*, 853.
[49] L. F. Sukhodub, *ChemInform.* **1987**, *18*, 589–606.
[50] I. K. Yanson, A. B. Teplitsky, L. F. Sukhodub, *Biopolymers* **1979**, *18*, 1149–1170.
[51] J. G. Contreras, S. T. Madariaga, *Bioorg. Chem.* **2003**, *31*, 367–377.
[52] K. Hoogsteen, *Acta. Crystallogr.* **1959**, *12*, 822–823.
[53] N. G. A. Abrescia, A. Thompson, T. Huynh-Dinh, J. A. Subirana, *Proc. Natl. Acad. Sci.* **2002**, *99*, 2806–2811.
[54] M. Kitayner, H. Rozenberg, R. Rohs, O. Suad, D. Rabinovich, B. Honig, Z. Shakked, *Nat. Struct. Mol. Biol.* **2010**, *17*, 423–429.
[55] P. A. Rice, S. Yang, K. Mizuuchi, H. A. Nash, *Cell* **1996**, *87*, 1295–1306.
[56] E. Cubero, F. J. Luque, M. Orozco, *Biophys. J.* **2006**, *90*, 1000–1008.
[57] E. Cubero, N. G. A. Abrescia, J. A. Subirana, F. J. Luque, M. Orozco, *J. Am. Chem. Soc.* **2003**, *125*, 14603–14612.
[58] E. Cubero, F. J. Luque, M. Orozco, *J. Am. Chem. Soc.* **2001**, *123*, 12018–12025.
[59] C. Escudé, S. Mohammadi, J.-S. Sun, C.-H. Nguyen, E. Bisagni, J. Liquier, E. Taillandier, T. Garestier, C. Hélène, *Chem. Biol.* **1996**, *3*, 57–65.
[60] G. M. Hashem, J.-D. Wen, Q. Do, D. M. Gray, *Nucleic Acids Res.* **1999**, *27*, 3371–3379.
[61] N. Escaja, I. Gómez-Pinto, M. Rico, E. Pedroso, C. González, *ChemBioChem.* **2003**, *4*, 623–632.
[62] V. Sklenář, J. Felgon, *Nature* **1990**, *345*, 836–838.
[63] K. Hoogsteen, *Acta. Crystallogr.* **1963**, *16*, 907–916.
[64] R. E. Johnson, L. Prakash, S. Prakash, *Proc. Natl. Acad. Sci.* **2005**, *102*, 10466–10471.
[65] J. Wang, *Nature* **2005**, *437*, E6–E7.
[66] L. Lu, C. Yi, X. Jian, G. Zheng, C. He, *Nucleic Acids Res.* **2010**, *38*, 4415–4425.
[67] D. T. Nair, R. E. Johnson, L. Prakash, S. Prakash, A. K. Aggarwal, *Structure* **2005**, *13*, 1569–1577.
[68] D. T. Nair, R. E. Johnson, S. Prakash, L. Prakash, A. K. Aggarwal, *Nature* **2004**, *430*, 377–380.
[69] V. Genna, E. Donati, M. De Vivo, *ACS Catal.* **2018**, *8*, 11103–11118.
[70] H. Ling, F. Boudsocq, B. S. Plosky, R. Woodgate, W. Yang, *Nature* **2003**, *424*, 1083–1087.
[71] I. Geronimo, P. Vidossich, E. Donati, M. De Vivo, *WIREs Comput. Mol. Sci.* **2021**, *11*, 1–26.
[72] G. A. Patikoglou, J. L. Kim, L. Sun, S.-H. Yang, T. Kodadek, S. K. Burley, *Genes Dev.* **1999**, *13*, 3217–3230.
[73] J. Aishima, *Nucleic Acids Res.* **2002**, *30*, 5244–5252.
[74] D. Golovenko, B. Bräuning, P. Vyas, T. E. Haran, H. Rozenberg, Z. Shakked, *Structure* **2018**, *26*, 1237-1250.e6.

[75] G. Ughetto, A. H. J. Wang, G. J. Quigley, G. A. van der Marel, J. H. van Boom, A. Rich, *Nucleic Acids Res.* **1985**, *13*, 2305–2323.
[76] A. Jain, G. Wang, K. M. Vasquez, *Biochimie* **2008**, *90*, 1117–1130.
[77] M. Duca, P. Vekhoff, K. Oussedik, L. Halby, P. B. Arimondo, *Nucleic Acids Res.* **2008**, *36*, 5123–5138.
[78] P. Yakovchuk, *Nucleic Acids Res.* **2006**, *34*, 564–574.
[79] E. T. Kool, *Annu. Rev. Biophys. Biomol. Struct.* **2001**, *30*, 1–22.
[80] C. H. Mak, *J. Phys. Chem. B.* **2016**, *120*, 6010–6020.
[81] S. Wärmländer, J. E. Sponer, J. Sponer, M. Leijon, *J. Biol. Chem.* **2002**, *277*, 28491–28497.
[82] S. Nakano, *Nucleic Acids Res.* **1999**, *27*, 2957–2965.
[83] S. H. Gellman, T. S. Haque, L. F. Newcomb, *Biophys. J.* **1996**, *71*, 3523–3525.
[84] P. O. P. Ts'o, I. S. Melvin, A. C. Olson, *J. Am. Chem. Soc.* **1963**, *85*, 1289–1296.
[85] P. Röthlisberger, C. Berk, J. Hall, *Chimia* **2019**, *73*, 368.
[86] X. Shen, D. R. Corey, *Nucleic Acids Res.* **2018**, *46*, 1584–1600.
[87] W. B. Wan, P. P. Seth, *J. Med. Chem.* **2016**, *59*, 9645–9667.
[88] I. V. Chernikov, V. V. Vlassov, E. L. Chernolovskaya, *Front Pharmacol.* **2019**, *10*, 1–25.
[89] C. Liczner, K. Duke, G. Juneau, M. Egli, C. J. Wilds, *Beilstein J. Org. Chem.* **2021**, *17*, 908–931.
[90] G. F. Deleavey, M. J. Damha, *Chem. Biol.* **2012**, *19*, 937–954.
[91] D. A. Brown, S. H. Kang, S. M. Gryaznov, L. DeDionisio, O. Heidenreich, S. Sullivan, X. Xu, M. I. Nerenberg, *J. Biol. Chem.* **1994**, *269*, 26801–26805.
[92] R. S. Geary, D. Norris, R. Yu, C. F. Bennett, *Adv. Drug Deliv. Rev.* **2015**, *87*, 46–51.
[93] M. Jayaraman, S. M. Ansell, B. L. Mui, Y. K. Tam, J. Chen, X. Du, D. Butler, L. Eltepu, S. Matsuda, J. K. Narayanannair, K. G. Rajeev, I. M. Hafez, A. Akinc, M. A. Maier, M. A. Tracy, P. R. Cullis, T. D. Madden, M. Manoharan, M. J. Hope, *Angew. Chem. Int. Ed.* **2012**, *51*, 8529–8533.
[94] M. Manoharan, *Biochimica et Biophysica Acta (BBA) - Gene Structure and Expression* **1999**, *1489*, 117–130.
[95] G. Das, S. Harikrishna, K. R. Gore, *The Chemical Record* **2022**, *22*, 1–27.
[96] A. Hendel, R. O. Bak, J. T. Clark, A. B. Kennedy, D. E. Ryan, S. Roy, I. Steinfeld, B. D. Lunstad, R. J. Kaiser, A. B. Wilkens, R. Bacchetta, A. Tsalenko, D. Dellinger, L. Bruhn, M. H. Porteus, *Nat. Biotechnol.* **2015**, *33*, 985–989.
[97] K. Fauster, C. Kreutz, R. Micura, *Angew. Chem. Int. Ed.* **2012**, *51*, 13080–13084.
[98] C. Höbartner, R. Micura, *J. Am. Chem. Soc.* **2004**, *126*, 1141–1149.
[99] K. Fauster, M. Hartl, T. Santner, M. Aigner, C. Kreutz, K. Bister, E. Ennifar, R. Micura, *ACS Chem. Biol.* **2012**, *7*, 581–589.
[100] C. V. Varaprasad, D. Averett, K. S. Ramasamy, J. Wu, *Tetrahedron* **1999**, *55*, 13345–13368.
[101] Y. F. Shealy, C. A. O'Dell, *J. Heterocycl. Chem.* **1976**, *13*, 1353–1354.
[102] S. Hoshika, *Nucleic Acids Res.* **2004**, *32*, 3815–3825.
[103] F. Kawasaki, P. Murat, Z. Li, T. Santner, S. Balasubramanian, *Chem. Commun.* **2017**, *53*, 1389–1392.
[104] Y. Kamiya, Y. Donoshita, H. Kamimoto, K. Murayama, J. Ariyoshi, H. Asanuma, *ChemBioChem.* **2017**, *18*, 1917–1922.
[105] M. Minuth, C. Richert, *Angew. Chem. Int. Ed.* **2013**, *52*, 10874–10877.
[106] I. Hirao, M. Kimoto, R. Yamashige, *Acc. Chem. Res.* **2012**, *45*, 2055–2065.
[107] Y. Doi, J. Chiba, T. Morikawa, M. Inouye, *J. Am. Chem. Soc.* **2008**, *130*, 8762–8768.
[108] M. Hocek, *Chem. Rev.* **2009**, *109*, 6729–6764.
[109] H. Liu, J. Gao, E. T. Kool, *J. Org. Chem.* **2005**, *70*.
[110] H. Liu, J. Gao, S. R. Lynch, Y. D. Saito, L. Maynard, E. T. Kool, *Science* **2003**, *302*.
[111] J. Gao, H. Liu, E. T. Kool, *Angew. Chem. Int. Ed.* **2005**, *44*.
[112] T. Carell, C. Brandmayr, A. Hienzsch, M. Müller, D. Pearson, V. Reiter, I. Thoma, P. Thumbs, M. Wagner, *Angew. Chem. Int. Ed.* **2012**, *51*, 7110–7131.

[113] M. Hocek, M. Fojta, *Chem. Soc. Rev.* **2011**, *40*, 5802.
[114] W. Xu, K. M. Chan, E. T. Kool, *Nat. Chem.* **2017**, *9*, 1043–1055.
[115] L. P. Jordheim, D. Durantel, F. Zoulim, C. Dumontet, *Nat. Rev. Drug Discov.* **2013**, *12*, 447–464.
[116] N. Tsesmetzis, C. B. J. Paulin, S. G. Rudd, N. Herold, *Cancers* **2018**, *10*, 240.
[117] J. Horlacher, M. Hottiger, V. N. Podust, U. Hübscher, S. A. Benner, *Proc. Natl. Acad. Sci.***1995**, *92*, 6329–6333.
[118] J. A. Piccirilli, S. A. Benner, T. Krauch, S. E. Moroney, S. A. Benner, *Nature* **1990**, *343*, 33–37.
[119] S. Katz, *Biochim. Biophys. Acta.* **1963**, *68*, 240–253.
[120] S. C. Rajasree, Y. Takezawa, M. Shionoya, *Chem. Commun.* **2023**, *59*, 1006–1009.
[121] K. Tanaka, A. Tengeiji, T. Kato, N. Toyama, M. Shiro, M. Shionoya, *J. Am. Chem. Soc.* **2002**, *124*, 12494–12498.
[122] J. Micklefield, *Curr. Med. Chem.* **2001**, *8*, 1157–1179.
[123] F. Eckstein, *Nucleic Acid Ther.* **2014**, *24*, 374–387.
[124] R. I. Hogrefe, M. M. Vaghefi, M. A. Reynolds, K. M. Young, L. J. Arnold, *Nucleic Acids Res.* **1993**, *21*, 2031–2038.
[125] A. Laurent, M. Naval, F. Debart, J.-J. Vasseur, B. Rayner, *Nucleic Acids Res.* **1999**, *27*, 4151–4159.
[126] B. R. Meade, K. Gogoi, A. S. Hamil, C. Palm-Apergi, A. van den Berg, J. C. Hagopian, A. D. Springer, A. Eguchi, A. D. Kacsinta, C. F. Dowdy, A. Presente, P. Lönn, M. Kaulich, N. Yoshioka, E. Gros, X.-S. Cui, S. F. Dowdy, *Nat. Biotechnol.* **2014**, *32*, 1256–1261.
[127] P. Röthlisberger, M. Hollenstein, *Adv. Drug Deliv. Rev.* **2018**, *134*, 3–21.
[128] D. A. Glazier, J. Liao, B. L. Roberts, X. Li, K. Yang, C. M. Stevens, W. Tang, *Bioconjug. Chem.* **2020**, *31*, 1213–1233.
[129] A. J. Berdis, *Chem. Rev.* **2009**, *109*, 2862–2879.
[130] K. Skarstad, S. Wold, *Mol. Microbiol.* **1995**, *17*, 825–831.
[131] M. F. Goodman, D. K. Fygenson, *Genetics* **1998**, *148*, 1475–1482.
[132] R. Mitra, B. M. Pettit, G. L. Rame`, R. D. Blake, *Nucleic Acids Res.* **1993**, *21*, 6028–6037.
[133] Y. Yuan, W. Wang, in Comprehensive Organic Synthesis: Second Edition, 2014.
[134] T. Ratvijitvech, R. Dawson, A. Laybourn, Y. Z. Khimyak, D. J. Adams, A. I. Cooper, *Polymer* **2014**, *55*, 321–325.
[135] G.-P. Li, K. Zhang, P.-F. Zhang, W.-N. Liu, W.-Q. Tong, L. Hou, Y.-Y. Wang, *Inorg. Chem.* **2019**, *58*, 3409–3415.
[136] C. S. Mahon, A. W. Jackson, B. S. Murray, D. A. Fulton, *Chem. Commun*. **2011**,*47*, 7209-7211.
[137] S. Mukherjee, W. L. A. Brooks, Y. Dai, B. S. Sumerlin *Polym. Chem*., **2016**,*7*, 1971-1978.
[138] M. R. Hill, S. Mukherjee, P. J. Costanzo, B. S. Sumerlin ***Polym. Chem.***, **2012**,***3***, 1758-1762
[139] D. W. Domaille, D. M. Love, X. Y. Rima, A. Harguindey, B. D. Fairbanks, D. Klug, J. N. Cha, C. N. Bowman, *Polym. Chem.*, **2018**, *9*, 3791-3797
[140] D. W. Domaille, J. N. Cha, *Chem. Commun*., **2014**,*50*, 3831-3833.
[141] K. L. Heredia, Z. P. Tolstyka, H. D. Maynard, *Macromolecules*, **2007**, *40*, 14, 4772–4779
[142] N. Vogel, P. Théato, *Macromol. Symp.* **2007**, 249–250, 383–391.
[143] A. Aho, M. Sulkanen, H. Korhonen, P. Virta, *Org. Lett.* **2020**, *22*, 17, 6714–6718
[144] D. A. Stetsenko, M. J. Gait, *J. Org. Chem.* **2000**, *65*, 4900–4908
[145] F. Amblard, J. H. Cho, R. F. Schinazi, *Chem. Rev.* **2009**, *109*, 4207–4220.
[146] D. Graham, A. Grondin, C. McHugh, L. Fruk, W. E. Smith, *Tetrahedron Lett.* **2002**, *43*, 4785–4788.
[147] S. H. Weisbrod, A. Marx, *Chem. Commun.* **2008**, 5675.
[148] A. Herrmann, *Chem. Soc. Rev.* **2014**, *43*, 1899–1933.
[149] M. Mondal, A. K. H. Hirsch, *Chem. Soc. Rev.* **2015**, *44*, 2455–2488.
[150] J. Li, P. Nowak, S. Otto, *J. Am. Chem. Soc.* **2013**, *135*, 9222–9239.
[151] J.-M. Lehn, *Chem. Soc. Rev.* **2007**, *36*, 151–160.

[152] B. Fuchs, *Isr. J. Chem.* **2013**, *53*, 45–52.
[153] B. de Bruin, P. Hauwert, J. N. H. Reek, *Angew. Chem. Int. Ed.* **2006**, *45*, 2660–2663.
[154] R. L. E. Furlan, S. Otto, J. K. M. Sanders, *Proc. Natl. Acad. Sci.* **2002**, *99*, 4801–4804.
[155] C. Karan, B. L. Miller, *Drug Discov Today* **2000**, *5*, 67–75.
[156] J. K. M. Sanders, *Chem. Eur. J.* **1998**, *4*, 1378–1383.
[157] P. A. Brady, J. K. M. Sanders, *Chem. Soc. Rev.* **1997**, *26*, 327.
[158] O. Ramstrom, *Biochimica et Biophysica Acta (BBA) - General Subjects* **2002**, *1572*, 178–186.
[159] B. Klekota, B. L. Miller, *Trends Biotechnol.* **1999**, *17*, 205–209.
[160] M. Sakulsombat, Y. Zhang, O. Ramström, in *Top Curr. Chem*. **2011**, pp. 55–86.
[161] K. Osowska, O. Miljanić, *Synlett* **2011**, *2011*, 1643–1648.
[162] V. del Amo, D. Philp, *Chem. Eur. J.* **2010**, *16*, 13304–13318.
[163] A. Vidonne, D. Philp, *Eur. J. Org. Chem.* **2009**, *2009*, 593–610.
[164] M. M. Rozenman, B. R. McNaughton, D. R. Liu, *Curr. Opin. Chem. Biol.* **2007**, *11*, 259–268.
[165] Z. J. Gartner, *Pure Appl. Chem.* **2006**, *78*, 1–14.
[166] A. Herrmann, *Chem. Eur. J.* **2012**, *18*, 8568–8577.
[167] S. Otto, K. Severin, in *Creative Chemical Sensor Systems*, Springer Berlin Heidelberg, Berlin, Heidelberg, **2007**, pp. 267–288.
[168] E. Moulin, G. Cormos, N. Giuseppone, *Chem. Soc. Rev.* **2012**, *41*, 1031–1049.
[169] A. Herrmann, *Org. Biomol. Chem.* **2009**, *7*, 3195.
[170] H. Y. Au-Yeung, F. B. L. Cougnon, S. Otto, G. D. Pantoş, J. K. M. Sanders, *Chem. Sci.* **2010**, *1*, 567.
[171] H. Y. Au-Yeung, G. D. Pantoş, J. K. M. Sanders, *J. Org. Chem.* **2011**, *76*, 1257–1268.
[172] N. Giuseppone, J. Lehn, *Chem. Eur. J.* **2006**, *12*, 1715–1722.
[173] V. A. Polyakov, M. I. Nelen, N. Nazarpack-Kandlousy, A. D. Ryabov, A. V. Eliseev, *J. Phys. Org. Chem.* **1999**, *12*, 357–363.
[174] A. Pross, *Chem. Eur. J.* **2009**, *15*, 8374–8381.
[175] P. Reutenauer, P. J. Boul, J. Lehn, *European J. Org. Chem.* **2009**, *2009*, 1691–1697.
[176] M. N. Chaur, D. Collado, J. Lehn, *Chem. Eur. J.* **2011**, *17*, 248–258.
[177] S. Di Stefano, M. Mazzonna, E. Bodo, L. Mandolini, O. Lanzalunga, *Org. Lett.* **2011**, *13*, 142–145.
[178] S. Fujii, J. Lehn, *Angew. Chem. Int. Ed.* **2009**, *48*, 7635–7638.
[179] N. Giuseppone, J. Schmitt, J. Lehn, *Angew. Chem. Int. Ed.* **2004**, *43*, 4902–4906.
[180] N. Hafezi, J.-M. Lehn, *J. Am. Chem. Soc.* **2012**, *134*, 12861–12868.
[181] J. M. A. Carnall, C. A. Waudby, A. M. Belenguer, M. C. A. Stuart, J. J.-P. Peyralans, S. Otto, *Science* **2010**, *327*, 1502–1506.
[182] S. K. M. Nalluri, R. V. Ulijn, *Chem. Sci.* **2013**, *4*, 3699.
[183] A. Herrmann, N. Giuseppone, J. Lehn, *Chem. Eur. J.* **2009**, *15*, 117–124.
[184] N. Giuseppone, J. Lehn, *Angew. Chem. Int. Ed.* **2006**, *45*, 4619–4624.
[185] B. Shi, R. Stevenson, D. J. Campopiano, M. F. Greaney, *J. Am. Chem. Soc.* **2006**, *128*, 8459–8467.
[186] A. M. Belenguer, T. Friščić, G. M. Day, J. K. M. Sanders, *Chem. Sci.* **2011**, *2*, 696.
[187] A. Bugaut, K. Jantos, J. Wietor, R. Rodriguez, J. K. M. Sanders, S. Balasubramanian, *Angew. Chem. Int. Ed.* **2008**, *47*, 2677–2680.
[188] A. J. Clipson, V. T. Bhat, I. McNae, A. M. Caniard, D. J. Campopiano, M. F. Greaney, *Chem. Eur. J.* **2012**, *18*, 10562–10570.
[189] R. J. Lins, S. L. Flitsch, N. J. Turner, E. Irving, S. A. Brown, *Angew. Chem. Int. Ed.* **2002**, *41*, 3405–3407.
[190] Z. Fang, W. He, X. Li, Z. Li, B. Chen, P. Ouyang, K. Guo, *Bioorg. Med. Chem. Lett.* **2013**, *23*, 5174–5177.
[191] H. Li, P. Williams, J. Micklefield, J. M. Gardiner, G. Stephens, *Tetrahedron* **2004**, *60*, 753–758.

[192] H. F. Nour, T. Islam, M. Fernández-Lahore, N. Kuhnert, *Rapid Commun. Mass Spectrom.* **2012**, *26*, 2865–2876.
[193] D. A. Erlanson, J. W. Lam, C. Wiesmann, T. N. Luong, R. L. Simmons, W. L. DeLano, I. C. Choong, M. T. Burdett, W. M. Flanagan, D. Lee, E. M. Gordon, T. O'Brien, *Nat. Biotechnol.* **2003**, *21*, 308–314.
[194] M. Hochgürtel, H. Kroth, D. Piecha, M. W. Hofmann, C. Nicolau, S. Krause, O. Schaaf, G. Sonnenmoser, A. V. Eliseev, *Proc. Natl. Acad. Sci.* **2002**, *99*, 3382–3387.
[195] N. R. Rose, E. C. Y. Woon, G. L. Kingham, O. N. F. King, J. Mecinović, I. J. Clifton, S. S. Ng, J. Talib-Hardy, U. Oppermann, M. A. McDonough, C. J. Schofield, *J. Med. Chem.* **2010**, *53*, 1810–1818.
[196] M. Demetriades, I. K. H. Leung, R. Chowdhury, M. C. Chan, M. A. McDonough, K. K. Yeoh, Y. Tian, T. D. W. Claridge, P. J. Ratcliffe, E. C. Y. Woon, C. J. Schofield, *Angew. Chem. Int. Ed.* **2012**, *51*, 6672–6675.
[197] N. Nazarpack-Kandlousy, J. Zweigenbaum, J. Henion, A. V. Eliseev, *J. Comb. Chem.* **1999**, *1*, 199–206.
[198] M. S. Congreve, D. J. Davis, L. Devine, C. Granata, M. O'Reilly, P. G. Wyatt, H. Jhoti, *Angew. Chem. Int. Ed.* **2003**, *42*, 4479–4482.
[199] I. K. H. Leung, M. Demetriades, A. P. Hardy, C. Lejeune, T. J. Smart, A. Szöllössi, A. Kawamura, C. J. Schofield, T. D. W. Claridge, *J. Med. Chem.* **2013**, *56*, 547–555.
[200] P. Vongvilai, M. Angelin, R. Larsson, O. Ramström, *Angew. Chem. Int. Ed.* **2007**, *46*, 948–950.
[201] M. Shibakami, M. Inagaki, S. L. Regen, *J. Am. Chem. Soc.* **1998**, *120*, 3758–3761.
[202] N. A. Stephenson, J. Zhu, S. H. Gellman, S. S. Stahl, *J. Am. Chem. Soc.* **2009**, *131*, 10003–10008.
[203] J. M. Hoerter, K. M. Otte, S. H. Gellman, Q. Cui, S. S. Stahl, *J. Am. Chem. Soc.* **2008**, *130*, 647–654.
[204] J. D. Cheeseman, A. D. Corbett, R. Shu, J. Croteau, J. L. Gleason, R. J. Kazlauskas, *J. Am. Chem. Soc.* **2002**, *124*, 5692–5701.
[205] R. Brachvogel, M. von Delius, *European J. Org. Chem.* **2016**, *2016*, 3662–3670.
[206] P. C. M. van Gerven, J. A. A. W. Elemans, J. W. Gerritsen, S. Speller, R. J. M. Nolte, A. E. Rowan, *Chem. Commun.* **2005**, 3535.
[207] A. González-Álvarez, I. Alfonso, V. Gotor, *Chem. Commun.* **2006**, 2224–2226.
[208] D. M. Epstein, S. Choudhary, M. R. Churchill, K. M. Keil, A. V. Eliseev, J. R. Morrow, *Inorg. Chem.* **2001**, *40*, 1591–1596.
[209] J. R. Nitschke, J.-M. Lehn, *Proc. Natl. Acad. Sci.* **2003**, *100*, 11970–11974.
[210] N. Nazarpack-Kandlousy, M. I. Nelen, V. Goral, A. V. Eliseev, *J. Org. Chem.* **2002**, *67*, 59–65.
[211] V. A. Polyakov, M. I. Nelen, N. Nazarpack-Kandlousy, A. D. Ryabov, A. V. Eliseev, *J. Phys. Org. Chem.* **1999**, *12*, 357–363.
[212] A. T. ten Cate, P. Y. W. Dankers, R. P. Sijbesma, E. W. Meijer, *J. Org. Chem.* **2005**, *70*, 5799–5803.
[213] J. Leclaire, L. Vial, S. Otto, J. K. M. Sanders, *Chem. Commun.* **2005**, 1959.
[214] R. L. E. Furlan, Y.-F. Ng, G. R. L. Cousins, J. E. Redman, J. K. M. Sanders, *Tetrahedron* **2002**, *58*, 771–778.
[215] R. Nguyen and Ivan Huc, *Chem. Commun.* **2003**, *8*, 942.
[216] P. J. Boul, P. Reutenauer, J.-M. Lehn, *Org. Lett.* **2005**, *7*, 15–18.
[217] B. Shi, M. F. Greaney, *Chem. Commun.* **2005**, 886.
[218] T. Giger, M. Wigger, S. Audétat, S. A. Benner, *Synlett.* **1998**, *1998*, 688–691.
[219] S. Ladame, *Org. Biomol. Chem.* **2008**, *6*, 219–226.
[220] S. Otto, R. L. E. Furlan, J. K. M. Sanders, *Drug Discov. Today* **2002**, *7*, 117–125.
[221] S. Otto, R. LE Furlan, J. K. Sanders, *Curr. Opin. Chem. Biol.* **2002**, *6*, 321–327.
[222] O. Ramström, J.-M. Lehn, *Nat. Rev. Drug Discov.* **2002**, *1*, 26–36.
[223] B. L. Miller, in *Top Curr. Chem*. **2011**, 107–137.
[224] D. T. Hickman, N. Sreenivasachary, J. Lehn, *Helv. Chim. Acta.* **2008**, *91*, 1–20.

[225] J. M. Heemstra, D. R. Liu, *J. Am. Chem. Soc.* **2009**, *131*, 11347–11349.
[226] Y. Liu, J.-M. Lehn, A. K. H. Hirsch, *Acc. Chem. Res.* **2017**, *50*, 376–386.
[227] D. M. Rosenbaum, D. R. Liu, *J. Am. Chem. Soc.* **2003**, *125*, 13924–13925.
[228] G. von Kiedrowski, *Angew. Chem. Int. Ed.* **1986**, *25*, 932–935.
[229] T. Inoue, G. F. Joyce, K. Grzeskowiak, L. E. Orgel, J. M. Brown, C. B. Reese, *J. Mol. Biol.* **1984**, *178*, 669–672.
[230] T. Wu, L. E. Orgel, *J. Am. Chem. Soc.* **1992**, *114*, 5496–5501.
[231] P. J. Unrau, D. P. Bartel, *Nature* **1998**, *395*, 260–263.
[232] B. A. Schweitzer, E. T. Kool, *J. Am. Chem. Soc.* **1995**, *117*, 1863–1872.
[233] L. E. Orgel, R. Lohrmann, *Acc. Chem. Res.* **1974**, *7*, 368–377.
[234] Y. Ura, J. M. Beierle, L. J. Leman, L. E. Orgel, M. R. Ghadiri, *Science* **2009**, 325, 73-77.
[235] Z. Kanlidere, O. Jochim, M. Cal, U. Diederichsen, *Beilstein J. Org. Chem*. **2016**, 12, 2136–2144.
[236] P. E. Nielsen, M. Egholm, R. H. Berg, O. Buchardt, *Science* **1991**, *254*, 1497–1500.
[237] F. R. Bowler, J. J. Diaz-Mochon, M. D. Swift, M. Bradley, *Angew. Chem. Int. Ed.* **2010**, *49*, 1809–1812.
[238] J. M. Heemstra, D. R. Liu, *J. Am. Chem. Soc.* **2009**, *131*, 11347–11349.
[239] P. E. Nielsen, M. Egholm, R. H. Berg, O. Buchardt, *Science* **1991**, *254*, 1497–1500.
[240] B. P. Sutherland, P. J. LeValley, D. J. Bischoff, A. M. Kloxin, C. J. Kloxin, *Chem. Commun.* **2020**, *56*, 11263–11265.
[241] J. Wallin, T. Lönnberg, *European J. Org. Chem.* **2022**, *2022*, 1–7.
[242] M. N. K. Afari, K. Nurmi, P. Virta, T. Lönnberg, *ChemistryOpen* **2023**, 12, 1–7.

TURUN
YLIOPISTO
UNIVERSITY
OF TURKU

Painosalama, Turku, Finland 2025

ISBN 978-952-02-0258-3 (PRINT)
ISBN 978-952-02-0257-6 (PDF)
ISSN 0082-7002 (Print)
ISSN 2343-3175 (Online)